

---

# ACTIVE LEARNING AND BAYESIAN OPTIMIZATION: A UNIFIED PERSPECTIVE TO LEARN WITH A GOAL

---

**Francesco Di Fiore**  
Politecnico di Torino  
francesco.difiore@polito.it

**Michela Nardelli**  
Politecnico di Torino  
michela.nardelli@polito.it

**Laura Mainini**  
Massachusetts Institute of Technology  
Politecnico di Torino  
laura.mainini@polito.it

March 6, 2023

## ABSTRACT

Both Bayesian optimization and active learning realize an adaptive sampling scheme to achieve a specific learning goal. However, while the two fields have seen an exponential growth in popularity in the past decade, their dualism has received relatively little attention. In this position paper, we argue for an original unified perspective of Bayesian optimization and active learning based on the synergy between the principles driving the sampling policies. This symbiotic relationship is demonstrated through the substantial analogy between the infill criteria of Bayesian optimization and the learning criteria in active learning, and is formalized for the case of single information source and when multiple sources at different levels of fidelity are available. We further investigate the capabilities of each infill criteria both individually and in combination on a variety of analytical benchmark problems, to highlight benefits and limitations over mathematical properties that characterize real-world applications.

## 1 Introduction

In science and engineering, one of the major challenge associated with the development of advanced technologies and systems is to satisfy competing objectives such as improving the overall performance and capabilities, while saving in computational resources and time. Almost invariably, this requires solving optimization problems through highly complicated and accurate representations of complex physical phenomena. The use of long running expensive computer simulations – e.g. Computational Fluid Dynamics (CFD) or Computational Structural Dynamics (CSD) – or physical experiments – e.g. lab-scale test benches or wind tunnel testing – leads to a significant hurdle: the demand for resources required to analyze all the combinations of optimization variables is difficult to be adequately satisfied. Indeed, the acquisition of data from these high-fidelity models involves huge non-trivial computational and economical cost resulting in the difficult computation of the analytical form of the objective function and its derivatives.

Historically, this motivates the growth of interest for surrogate models – also referred to as meta models or response surfaces – capable to predict the output of expensive computer codes or real-world experiments at untried points of the domain with contained computational cost [1, 2, 3]. Accordingly, Surrogate-Based Optimization (SBO) has attracted significant attention in science and engineering, where the request for high-fidelity data might be particularly intense to address large-scale design optimization problems. Many researchers from different fields of expertise observed that surrogate-based optimization is potentially an effective methodology, and this is predominantly for the capability of surrogate models to accelerate the search for optimal solutions and reduce the sampling requirements. Queipo et al. [4] discuss the adoption of surrogate models to reduce the computational cost associated with expensive optimization problems, motivated by the application to complex aerospace systems. Wang and Shan [5] overview a variety of surrogate models techniques, dedicating particular attention to global optimization and multi-objective optimization. Haftka et al. [6] detail strategies for global optimization using surrogate models, with main focus on criteria for local and global searches from the perspective of parallelization. Examples of applications of SBO include and are not limited to the optimization of aircraft wings [7], rocket engines [8], production of materials [9], clinical and medical devices [10], autonomous vehicles [11], and vessels [12].

Surrogate models are computed starting from data acquired evaluating the responses of models that are treated as black-box information sources. This scenario is typical in science and engineering, where the input/output relationship that characterizes the models of the objective function is depicted through computer simulations or laboratory experiments, and is not directly accessible to the optimizer. The performance of SBO is deeply influenced by the sampling scheme adopted to build the surrogate model since it contributes to the overall fitting accuracy and computational cost that raise from the evaluations of the objective function. To ensure the accuracy and efficiency of the surrogate while containing the sampling expenditure, a multitude of sampling schemes have been developed in literature. Among these, adaptive methods [13] provide an efficient goal-driven approach where the surrogate model is progressively learned evaluating the objective function in prescribed points of the domain, targeting either the improvement of the fitting quality across the domain or the acceleration of the search and identification of optimal solutions [14, 15, 16]. This permits to develop an objective oriented procedure that aims at reducing the number of evaluations of the objective function, selecting only the more informative samples according to certain criteria defined to accomplish the goal.

Bayesian Optimization (BO) is an established methodology to solve expensive optimization problems through an adaptive sampling scheme that seeks to realize a resource efficient identification of optimal solutions [17, 18]. BO techniques build up from the works of Kushner [19], Zhilinskas [20] and Moćkus [21], and gained popularity across a multitude of research communities in engineering through the Efficient Global Optimization algorithm developed by Jones et al. [22]. Bayesian optimization specifies the belief over possible explanations for the objective function by learning a surrogate model, and then computes an acquisition function that combines this belief to measure the utility of promising queries. The acquisition function is driven by infill criteria realizing a goal-driven adaptive sampling scheme that guides the search based on the prediction of the surrogate, and is responsible for quantifying the merit of unknown samples in terms of improvement of the solution of the optimization problem.

The most popular paradigms for Bayesian optimization highlight a substantial synergy with the field of active learning that is not explicitly accounted in literature, precluding new research avenues and opportunities that could be tracked through collaboration between researchers in both spheres. Active learning (AL) is a family of machine learning techniques where the learner is capable to select the training data according to an adaptive sampling strategy that maximizes the learning performance to achieve a specified goal [23]. This goal in AL is usually computing an accurate model with the minimum computational cost and using a reduced number of samples [24]. In particular, pool-based active learning [25] approaches present a remarkable analogy – not currently well investigated – with the Bayesian optimization approach. In pool-based AL, the distribution of labels is unknown and is predicted through a classification model – which can be seen as the conceptual analogous of the surrogate model in BO – computed on a given small pool of input samples from this distribution. The active learner defines an adaptive sampling procedure which selects the best training samples to improve the overall accuracy of the model over the space of samples. Pool-based AL shows a strong analogy with BO where the distribution of the objective function is not known a priori and the acquisition function guides the query of promising samples to either compute an accurate surrogate model or determine optimal solution of optimization problem.

This position paper proposes an original perspective of Bayesian optimization and active learning as symbiotic expressions of adaptive sampling introducing a unifying viewpoint based on common principles. In particular, we elucidate this synergy through a unified formulation of both spheres in the case of a single source providing the information about samples to accomplish the learning goal – Bayesian optimization and active learning –, and when multiple sources of information are available and ordered according to a hierarchy of fidelity in terms of accuracy and cost known a priori – multifidelity Bayesian optimization and active learning with multiple oracles. This unified interpretation is based on the dualism between the acquisition function and the active learner as the elements responsible for deciding how to adaptively learn from samples. Accordingly, we review and analyze popular formulations of the acquisition function for Bayesian optimization and multifidelity Bayesian optimization emphasizing the different infill criteria to quantify the expected utility of unknown samples, and demonstrate the analogy with the learning criteria that characterize active learning frameworks with single and multiple oracles.

In addition, this paper investigates Bayesian optimization as an active learning process comparing the performance of well established Bayesian techniques based on acquisition functions – considering both single-fidelity and multifidelity formulations – realizing sampling schemes driven by the learning principles in common across the two fields. This is realized through a set of benchmark problems identified by an international community of researchers to stress test goal-driven learning schemes, and validate the algorithms against a multitude of mathematical properties traceable in real-world optimization problems [26]. The objective of the benchmarking study is to provide awareness about the capabilities of different learning criteria, and illustrate opportunities and limitations in addressing challenging features of optimization problems that are frequently encountered in complex scientific and engineering applications.

This manuscript is organized as follows. Section 2 provides an overview on Bayesian optimization and multifidelity Bayesian optimization. Section 3 presents our perspective on the symbiotic relationship between Bayesian optimiza-

tion and active learning. Then, in Section 4 popular Bayesian optimization and multifidelity Bayesian optimization algorithms are numerically investigated over a variety of benchmark problems. Finally, Section 5 provides concluding remarks.

## 2 Background

### 2.1 Bayesian Optimization

The birth of Bayesian optimization can be retraced in 1964 with the work of Kushner [19] where unconstrained one-dimensional optimization problems are addressed through a predictive framework based on the Wiener process surrogate model, and a sampling scheme guided by the probability of improvement acquisition function to select the most promising sample to query. Further contributions have been proposed by Zhilinskas [20] and Mockus [21], and the methodology has been extended to high dimensional optimization problems in the works of Stuckman [27] and Elder [28]. Bayesian optimization achieved resounding success after the introduction of the Efficient Global Optimization (EGO) algorithm by Jones et al. [22]. EGO uses a Kriging model to predict the distribution of the objective function, and adopts the expected improvement acquisition function to measure the improvement of the optimization procedure obtained evaluating unknown samples.

The EGO methodology paves the way to the application of Bayesian optimization over a wide range of problems in science and engineering. Aerospace engineering has been pioneer in the adoption of Bayesian optimization [29] since the design of aerospace vehicles demand for the expensive joint optimization of structural and aerodynamic capabilities, propulsion efficiency, safety and competitiveness. Accordingly, Bayesian optimization has been both a need and an opportunity to efficiently identify optimal design solutions for demanding decision-making aerospace problems [30]. First examples of BO applications are in the design optimization of multi-element airfoils configurations [31], and in the aerodynamic shape optimization of two-dimensional airfoils [32]. Nowadays, the Bayesian framework becomes widely adopted in many fields including and not limited to aerospace engineering [33], chemical [34] and material sciences [35], electric vehicles [36] and robotics [37] design.

Given a black-box expensive objective function  $f : \mathcal{X} \rightarrow \mathbb{R}$ , Bayesian optimization seeks to identify the input  $\mathbf{x}^* \in \min_{\mathbf{x} \in \mathcal{X}} f(\mathbf{x})$  that minimizes the objective  $f$  over an admissible set of queries  $\mathcal{X}$  with a reduced computational cost. To achieve this goal, Bayesian optimization relies on an adaptive sampling scheme based on a surrogate model that provides a probabilistic representation of the objective  $f$ , and uses this information to compute an acquisition function  $U(\mathbf{x}) : \mathcal{X} \rightarrow \mathbb{R}^+$  that drives the selection of the most promising sample to query. Let us consider the available information regarding the objective function  $f$  stored in the dataset  $\mathcal{D}_N = \{(\mathbf{x}_1, y_1), \dots, (\mathbf{x}_n, y_n)\}$  where  $y_n \sim \mathcal{N}(f(\mathbf{x}_n), \sigma_\epsilon(\mathbf{x}_n))$  are the noisy observations of the objective function and  $\sigma_\epsilon$  is the standard deviation of the normally distributed noise.

At each iteration of the optimization procedure, the surrogate model depicts possible explanations of  $f$  as  $f \sim p(f|\mathcal{D}_N)$  applying a joint distribution over its behaviour at each sample  $\mathbf{x} \in \mathcal{X}$ . Typically, Gaussian Processes (GPs) have been widely used as the surrogate model for Bayesian optimization [38, 39]. In GP regression, the prior distribution of the objective  $p(f)$  is combined with the likelihood function  $p(\mathcal{D}_N|f)$  to compute the posterior distribution  $p(f|\mathcal{D}_N) \propto p(\mathcal{D}_N|f)p(f)$ , representing the updated beliefs about  $f$ . The GP posterior is a joint Gaussian distribution  $p(f|\mathcal{D}_N) = \mathcal{N}(\boldsymbol{\mu}(\mathbf{x}), \boldsymbol{\kappa}(\mathbf{x}, \mathbf{x}'))$  completely specified by its mean  $\boldsymbol{\mu}(\mathbf{x}) = \mathbb{E}[f(\mathbf{x})]$  and covariance (also referred as kernel) function  $\boldsymbol{\kappa}(\mathbf{x}, \mathbf{x}') = \mathbb{E}[(f(\mathbf{x}) - \boldsymbol{\mu}(\mathbf{x}))(f(\mathbf{x}') - \boldsymbol{\mu}(\mathbf{x}'))]$ , where  $\boldsymbol{\mu}(\mathbf{x})$  represents the prediction of the GP model at  $\mathbf{x}$  and  $\boldsymbol{\kappa}(\mathbf{x}, \mathbf{x}')$  the associated uncertainty.

BO uses this statistical belief to make the decision of where to sample assisted by an acquisition function  $U$  that identifies the most informative sample  $\mathbf{x}_{new} \in \mathcal{X}$  that should be evaluated via maximization  $\mathbf{x}_{new} \in \max_{\mathbf{x} \in \mathcal{X}} U(\mathbf{x})$ . Then, the objective function is evaluated at  $\mathbf{x}_{new}$  and this information is used to update the dataset  $\mathcal{D}_N = \mathcal{D}_N \cup (\mathbf{x}_{new}, y(\mathbf{x}_{new}))$ . Acquisition functions are designed to guide the search for the optimum solution according to different infill criteria providing a measure of the improvement that the next query is likely to provide with respect to the current posterior distribution of the objective function. In engineering applications, we could retrieve different implementations proposed for the acquisition function, which differ for the infill schemes adopted to sample pursuing the optimization goal. Examples include the Probability of Improvement (PI) [40], Expected Improvement (EI) [22], Entropy Search (ES) [41] and Max-Value Entropy Search (MES) [42], Knowledge-Gradient (KG) [43], and non-myopic acquisition functions [44, 45].

The Probability of Improvement (PI) acquisition function encourages the selection of samples that are likely to obtain larger improvements over the current minimum predicted by the surrogate model, while the Expected Improvement (EI) considers not only the PI but also the expected gain in the solution of the optimization problem achieved evaluating a certain sample. Other popular schemes are entropy-based acquisition functions such as the Entropy Search (ES) and Max-Value Entropy Search (MES), which rely on estimating the entropy of the location of the optimum and the

minimum function value, respectively, to maximize the mutual information between the samples and the location of the global optimum. Knowledge-gradient sampling procedures are conceived for applications where the evaluations of the objective function are affected by noise, recommending the location that maximizes the increment of the expected value that would be acquired by taking a sample from the location. Through the adoption of non-myopic acquisition functions, the optimizer selects the sample that maximizes the improvement at future iterations of the optimization procedure overcoming myopic schemes where the improvement of the solution is measured at the immediate step ahead. Differently from the objective function, the acquisition functions can be computed with a reduced computational cost and might be maximized through a derivative-free global optimization strategy [46] or a gradient-based local optimizer [47].

## 2.2 Multifidelity Bayesian Optimization

The Bayesian framework demands for the evaluation of several observations of the objective function – potentially in the order of tens of thousands for high-dimensional design optimization problems in engineering – to identify optimal solutions, leading to unfeasible computational cost for large-scale optimization problems where the evaluation of the objective function requires time-consuming lab experiments or expensive computer-based models. In many real-world applications, the objective function can be computed using multiple representations at different levels of fidelity  $\{f^{(1)}, \dots, f^{(L)}\}$ , where the lower the level of fidelity the less accurate but also less time-consuming the evaluation procedure. Multifidelity methods have emerged as powerful strategies to enable a flexible trade-off between the computational cost for optimization and the accuracy of the solution, leveraging low-fidelity data to massively query the input space and using a reduced number of high-fidelity observations to refine the belief about the objective function toward the optimum [48, 49, 50]. Accordingly, Multifidelity Bayesian Optimization (MFBO) learns a multifidelity surrogate model providing a stochastic approximation of the objective function for each level of fidelity, and defines an adaptive sampling scheme through a multifidelity acquisition function that permits to query the objective selecting the most promising sample location and the associated level of fidelity to be invoked.

Similarly to the single-fidelity framework, first applications of multifidelity Bayesian optimization are traceable in the aerospace field, where it has been adopted for the design optimization of a transonic civil aircraft wing [51], for the identification of the optimal mass flow for hypersonic vehicle design [52] and for supersonic aerodynamic design optimization [53]. Further, this technique has been applied to the large-scale multidisciplinary design optimization problems of high altitude and long endurance aircraft [54]. In recent years, multifidelity Bayesian optimization has been successfully adopted for optimization problems ranging from marine engineering [55] to material science [56], from reinforcement learning [57] to hyperparameter tuning [58], and from cyber-physical systems [59] to medical applications [60].

In the multifidelity setting, the information of the objective function extracted from multiple sources are collected into a dataset  $\mathcal{D}_N = \{(\mathbf{x}_1, y_1^{(l_1)}), \dots, (\mathbf{x}_n, y_n^{(l_n)})\}$  where  $y_n^{(l_n)} \sim \mathcal{N}(f^{(l_n)}(\mathbf{x}_n), \sigma_\varepsilon(\mathbf{x}_n))$  and  $\sigma_\varepsilon$  have the same distribution over the fidelities. Similarly to BO, the multifidelity surrogate model defines at each iteration an approximation of  $f^{(l)}$  as  $f^{(l)} \sim p(f^{(l)} | (\mathbf{x}, l), \mathcal{D}_N)$  for each  $l$ -th level of fidelity, representing our belief about the distribution of the objective function in the domain  $\chi$  at different levels of fidelity. A popular practice for MFBO is to extend the Gaussian process surrogate model to a multifidelity setting through an autoregressive scheme [61]:

$$f^{(l)} = \rho f^{(l-1)}(\mathbf{x}) + \zeta^{(l)}(\mathbf{x}) \quad l = 2, \dots, L \quad (1)$$

where  $\rho$  is a constant scaling factor that includes the contribution of the previous fidelity with respect to the following one, and  $\zeta^{(l)} \sim GP(0, \kappa^{(l)}(\mathbf{x}, \mathbf{x}'))$  models the discrepancy between two adjoining levels of fidelity. The posterior of the multifidelity Gaussian process is completely specified by the multifidelity mean function  $\mu^{(l)}(\mathbf{x}, l) = \mathbb{E}[f^{(l)}(\mathbf{x})]$  that represents the approximation of the objective function at different levels of fidelity, and the multifidelity covariance function  $\kappa^{(l)}((\mathbf{x}, l), (\mathbf{x}', l)) = \mathbb{E}[(f^{(l)}(\mathbf{x}, l) - \mu^{(l)}(\mathbf{x}, l))(f^{(l)}(\mathbf{x}', l) - \mu^{(l)}(\mathbf{x}', l))]$  that defines the associated uncertainty for each level of fidelity.

The availability of multiple representations of the objective function poses a further decisional task that has to be accounted during the sampling of unknown locations: the selection of the most promising sample is effected with the simultaneous designation of the information source to be evaluated. This is obtained through an adaptive sampling scheme driven by the multifidelity acquisition function  $U(\mathbf{x}, l)$  that extends the infill criteria of Bayesian optimization, and selects the pair of sample and the associated level of fidelity to query  $(\mathbf{x}_{new}, l_{new}) \in \max_{\mathbf{x} \in \chi, l \in \mathcal{L}} U(\mathbf{x}, l)$  that is likely to provide higher gains with a regard for the computational expenditure. Among different formulations, well known multifidelity acquisition functions to address optimization problems are the Multifidelity Probability of Improvement

(MFPI) [62], Multifidelity Expected Improvement (MFEI) [63], Multifidelity Predictive Entropy Search (MFPES) [64], Multifidelity Max-Value Entropy Search (MFMES) [65], and non-myopic multifidelity expected improvement [66]. These formulations of the acquisition function define adaptive sampling schemes that retain the infill principles characterizing the single-fidelity counterpart, and account for the dual decision task balancing the accuracy achieved through accurate queries with the associated cost during the optimization procedure. As for the acquisition function in BO, the evaluation of the multifidelity acquisition function is not computationally intensive and its maximization can be accomplished adopting the same techniques reported in Section 2.1.

### 3 An Active Learning Perspective

Across the machine learning community, Bayesian optimization and multifidelity Bayesian optimization are regarded as sample-efficient computational techniques for the optimization of black-box objective functions where the adaptive sampling scheme defined by the acquisition function guides the search to accomplish a specific learning goal. Bayesian frameworks exhibit a strong synergy – currently not explicitly established – with the concept of active learning. Indeed, Active Learning (AL) paradigms define a sampling procedure which, in principle, represent also an adaptive sampling similar to the one realized by acquisition functions in Bayesian strategies: the learner seeks to design an efficient sampling policy targeting the improvement of the accuracy of the model that approximates the behaviour of the overall samples while containing the queries at minimum.

Active learning techniques include a multitude of approaches [67, 68, 69, 70, 71, 72, 73, 74] that are commonly classified according to the nature of the sampling scheme defined by the learner. We follow the classification proposed by Sugiyama and Nakajima [75], and categorize the active learning approaches according to the query procedure into population-based and pool-based active learning frameworks. Population-based active learning considers available the distribution of the inputs and the learner can query any sample available. The learner pursues the goal of identifying the best optimal density of the inputs to generate the more efficient set of training samples. Conversely, in pool-based active learning the distribution of the inputs is unknown but a pool of samples from this distribution is given. The learning objective is the optimal selection of samples that allows to compute an effective model capable to represent the remaining samples with a high degree of accuracy.

Pool-based active learning shows in essence a strong analogy with the learning procedure adopted in Bayesian frameworks. These techniques seek to construct a model that represents the class of all the admissible unknown queries  $\chi = \{\mathbf{x}_1, \dots, \mathbf{x}_U\}$  given a contained amount of known samples  $\mathcal{D}_N = \{(\mathbf{x}_1, f_1), \dots, (\mathbf{x}_n, f_n)\}$ , where  $\mathbf{x} \in \mathbb{R}^D$  is the  $D$ -dimensional vector of the features and  $f \in \mathbb{R}$  is the class label. Similarly to Bayesian optimization, the learner sequentially selects an unlabeled data  $\mathbf{x}_i$  from  $\chi$  and queries its label  $f_i$  through an oracle. This query is tailored to achieve the goal of improving the accuracy of the model while using only a limited and well selected amount of informative samples for the training process. This learning procedure is of the nature of Bayesian optimization where the distribution of the objective function is not known a priori, and the acquisition function guides the query of promising samples to accomplish the goal of either compute an accurate surrogate model or the identification of optimal solutions.

This paper explicitly establishes the dualism of Bayesian frameworks as an active learning procedure realized through acquisition functions. In particular, we bring to light this synergy analyzing the learning criteria that guide the adaptive sampling in pool-based active learning, and demonstrate that these principles are also impersonated by the infill criteria that guide the adaptive search paradigms realized by the acquisition functions. This symbiosis is evidenced for the case of a single source of information adopted to query unknown samples, and when multiple sources are at disposal of the learner to interrogate new input. Accordingly, we review and discuss the sampling strategies commonly adopted in pool-based active learning frameworks, and discern from these approaches the learning criteria that realize the adaptive queries to accomplish a specific learning goal (Section 3.1). Then, the attention is dedicated to the explicit identification of the infill criteria realized through popular acquisition functions in Bayesian optimization (Section 3.2), namely the expected improvement, probability of improvement, entropy search and max-value entropy search. The objective is to compare these infill principles with the learning criteria in pool-based active learning, and explicitly formulate the synergy between Bayesian frameworks and Active learning as adaptive sampling schemes guided by common principles. The same avenue is followed to formalize the synergy for the case of multiple sources of information available for querying during the sampling procedure. In particular, we identify the learning criteria that guide the sampling process for active learning with multiple oracles (Section 3.3), and compare them with the infill criteria specified by well-established multifidelity acquisition functions in multifidelity Bayesian optimization (Section 3.4). This permits to clarify the shared principles and the mutual relationship that characterize the two adaptive sampling schemes, when the decision of the sample to query requires also the selection of the appropriate source of information to be evaluated.

### 3.1 Learning Criteria

The vast majority of the literature concerning pool-based active learning identifies three essential learning criteria that drive the adaptive sampling: informativeness, representativeness and diversity [76, 77, 78, 74, 79, 80]. Informativeness represents the amount of information achievable evaluating a certain sample to reduce the uncertainty associated with the model and contain the generalization error. Representativeness constitutes the capability of samples to exploit the structure underlying unknown samples, quantifying the similarity between a certain target sample and the neighboring samples. Diversity denotes that the selected sample should scatter across the full input space instead of concentrating in small local regions. With the purpose of highlighting how the learning criteria are implemented into the querying strategy to determine the most useful sample to interrogate, the remaining of this section is dedicated to the revision and discussion of popular pool-based active learning sampling schemes.

The first category of sampling strategies are uncertainty-based policies: the aim is to select the sample characterized by the largest uncertainty to improve the overall accuracy of the model, defining a sampling procedure driven by the informativeness learning criteria. Popular uncertainty-based strategies are uncertainty sampling algorithms that query the most promising sample according to the highest uncertainty in the predicted label [81] and its alternatives as margin-based [82], least confident [83] and entropy-based [84]. In a similar fashion, other strategies target the reduction of the uncertainty of the model selecting the point that allows to minimize the predicted variance [85], to maximize the decrease of loss augmenting the training set [23], and to maximize the gradient descend [86]. Another popular uncertainty-based approach is the query-by-committee sampling where a committee of models computed on a subset of the unknown locations are used to predict labels, selecting the most informative location as the one characterized by the largest disagreement between predictions of the committee [68, 87]. The major limitation of Uncertainty-based policies is the missing of information about the prediction of the model during the learning process, which in turn makes straightforward the implementation and efficient the computations but limits the overall performance and robustness to outliers.

Another popular class of pool-based active learning approaches are representative/diversity-based algorithms, which measure the goodness of samples according to the capability of representing a pool of unknown locations that maximizes the overall training utility. This category includes a multitude of algorithms that can be summarized in two main approaches: clustering methodology and optimal experimental design. The clustering technique exploits the underlying structure of unknown locations to determine the most informative points as the one closest to the cluster centers. Popular clustering strategies are hierarchical clustering [88], where the representativeness of samples is measured according to the information provided by the clusters, and k-center clustering that determines a subset of k congruent clusters that together cover the sampling space and whose radius is minimized [89]. Optimal experimental design defines a sampling scheme where the most representative sample is queried through the optimization of the selection process. This is achieved exploiting the information acquired from a prior representation to provide as much information as possible on the parameters of the model [90, 91, 92]. The main advantage of representative/diversity-based active learning is the capability to grasp information from unknown data overcoming the potential issue of uncertainty-based strategies. However, both clustering and experimental design methods come with significant disadvantages: the performance of the clustering approach is sensitive to how well the highlighted structures can represent the structure of the entire dataset, while the main problem of experimental design is that requires a large number of samples to determine the optimal decision boundary.

To overcome the limitations of uncertainty- and representative/diversity-based approaches, combined-based algorithms have been proposed to leverage the integration of multiple learning criteria targeting the improvement of the overall sampling performance. According to the literature [93, 80], combined algorithms are classified in three main categories based on the integrative approach, namely serial-form, criteria selection, and parallel-form strategies. Serial-form algorithms select the most promising location to query adopting sequentially the uncertainty sampling to determine an informative subset of data, and then using the clustering approach on this subset to identify the centers of the cluster as the samples to interrogate [77]. Criteria selection strategies maximize a selection parameter that at each iteration drives the selection of the appropriate sampling criterion through a measurement of the learning improvement [94]. Parallel-form methods seek to combine simultaneously multiple learning criteria through multi-objective optimization strategies to get full advantage of the features and compensate for the weaknesses that characterize each learning criteria [95, 96, 97].

### 3.2 Acquisition Functions and Infill Criteria

The identification of the learning criteria that drive the selection of promising samples in active learning permits to explicitly define the synergy with the sampling scheme realized in Bayesian optimization frameworks. In particular, the symbiotic relationship between the two domains is manifested in the substantial analogy between the infill criteria in Bayesian optimization and the learning criteria in active learning schemes. Infill criteria guide the sampling procedure

in Bayesian frameworks assessing the utility of evaluating an unknown sample to maximize the informative gain related to a specific optimization problem. The merit of each candidate is quantified according to a learning goal that establishes an adaptive sampling scheme realized through the acquisition function. The acquisition function  $U(\mathbf{x})$  embeds and formalizes the infill criteria measuring the improvement of the solution of the optimization problem, and enabling to decide the most promising sample  $\mathbf{x}$  and consequently where to expensively evaluate the objective function  $f$ .

Acquisition functions define the sampling process targeting the balance between two infilling criteria: the global exploration and the local exploitation toward the believed optimum. Specifically, the exploration concentrates the sampling on the regions where the predicted uncertainty about the objective function is larger, improving the knowledge about the distribution of  $f$  over the feasible set  $\mathcal{X}$ ; the exploitation condensates the sampling on regions where the minimum of the mean prediction is located to rapidly assess the optimal solution. The dilemma between exploration and exploitation of the search space represents a key challenge to be carefully addressed in formulating acquisition functions. On the one hand, a strategy that only explores data may not account for informative regions of the input space where sampling can improve the solution of the optimization problem. On the other hand, the pure exploitation of data may not consider large regions of the input space leading to a surrogate model locally accurate but globally incorrect. These extreme behaviours demonstrate the need to find a compromise between exploration and exploitation criteria.

In principle, these infill criteria are strongly related to the learning criteria commonly adopted in active learning: the concept of exploration is close to the informativeness criteria since both address the increase of the awareness about the objective function or the accuracy of the predictive model, while exploitation and representativeness/diversity criteria share the same concept of sampling in area already populated with observed samples to determine the local optimum or locally refine the predictive model. The following sections are dedicated to the revision of three popular acquisition functions commonly adopted in Bayesian frameworks, namely the expected improvement, probability of improvement, and max-value entropy search. This permits to discuss the formalization of the infill criteria identifying the symbiotic aspects with learning criteria in active learning, highlighting how both Bayesian optimization and active learning define sampling schemes driven by the same principles.

### 3.2.1 Expected Improvement

The Expected Improvement (EI) acquisition function quantifies the expected value of the improvement in the solution of the optimization problem achieved evaluating a certain location of the domain [22, 98]. EI at the generic location  $\mathbf{x}$  relies on the predicted improvement over the best solution of the optimization problem observed so far. Considering the GP as the surrogate model, EI can be expressed as follows:

$$U_{EI}(\mathbf{x}) = \sigma(\mathbf{x})(I(\mathbf{x})\Phi(I(\mathbf{x}))) + \mathcal{N}(I(\mathbf{x}); 0, 1) \quad (2)$$

where  $I(\mathbf{x}) = (f(\hat{\mathbf{x}}^*) - \mu(\mathbf{x}))/\sigma(\mathbf{x})$  is the predicted improvement,  $\hat{\mathbf{x}}^*$  is the current location of the best value of the objective sampled so far,  $\Phi(\cdot)$  is the cumulative distribution function of a standard normal distribution,  $\mu$  is the mean function and  $\sigma$  is the standard deviation of the GP. The computation of  $U_{EI}(\mathbf{x})$  requires limited computational resources and the first-order derivatives are easy to calculate:

$$\frac{\partial U_{EI}(\mathbf{x})}{\mu(\mathbf{x})} = -\Phi(I(\mathbf{x})) \quad (3)$$

$$\frac{\partial U_{EI}(\mathbf{x})}{\sigma(\mathbf{x})} = \phi(I(\mathbf{x})). \quad (4)$$

Both Equation (3) and Equation (4) demonstrate that  $U_{EI}(\mathbf{x})$  is monotonic with respect to the increase of both the mean and the uncertainty of the GP surrogate model. This highlights a form of trade-off between exploration and exploitation in the formulation of EI: the goal is to balance the sampling in locations of the domain where is likely to have a significant predicted improvement with respect to the current best solution, and the observations of regions where the improvement is contained but the prediction is highly uncertain. In principle, it is possible to affirm that EI follows both the informativeness and representativeness/diversity criteria adopted in active learning since tries to learn the minimum of the objective function with a continuous trade-off between the reduction of the uncertainty of the surrogate model and the sampling in explored regions where is likely to find the minimum of the objective function.

### 3.2.2 Probability of Improvement

The Probability of Improvement (PI) acquisition function targets the locations characterized by the highest probability of improving the objective function relying on the information from the current surrogate model [40, 99]. PI measures the probability that the prediction of the surrogate model at the generic location is lower than the best observation of the objective function so far. Under the Gaussian process surrogate model, the PI acquisition function is computed in closed form as follows:

$$U_{PI}(\mathbf{x}) = \Phi(I(\mathbf{x})) \quad (5)$$

where  $\Phi(\cdot)$  is the cumulative distribution function of a standard normal distribution and  $\mathbf{x}^*$  is the current location of the best value of the objective. Similarly to EI, also  $U_{PI}(\mathbf{x})$  is inexpensive to compute and the evaluation of the first-order derivatives requires simple calculations:

$$\frac{\partial U_{PI}(\mathbf{x})}{\partial \mu(\mathbf{x})} = -\frac{1}{\sigma(\mathbf{x})} \phi(I(\mathbf{x})) \quad (6)$$

$$\frac{\partial U_{PI}(\mathbf{x})}{\partial \sigma(\mathbf{x})} = -\frac{I(\mathbf{x})}{\sigma(\mathbf{x})} \phi(I(\mathbf{x})) \quad (7)$$

where  $\phi$  is the standard Gaussian probability density function. As demonstrated by Equation (6), regions of the input space characterized by lower values of the posterior mean of the GP are preferred for sampling, at fixed uncertainty of the surrogate. Moreover, Equation (7) shows that if  $\mu(\mathbf{x}) < f(\mathbf{x}^*)$  the regions characterized by lower uncertainty are preferred and, conversely, PI increases with uncertainty. Overall, the PI acquisition function can be considered as an exploitative scheme that determines the most informative location as the one that potentially produces a larger reduction of the minimum value of the objective function observed so far, sampling regions already explored where the surrogate model is reliable and characterized by lower levels of uncertainty. In principle, this sampling scheme makes PI in accordance with the representativeness/diversity learning criteria in active learning since the search toward the optimum is directed in known locations where the minimum is likely to be located.

### 3.2.3 Entropy Search and Max-value Entropy Search

The Entropy Search (ES) acquisition function measures the differential entropy of the believed location of the global minimum of the objective function, targeting the samples that allow to obtain the maximum decrease of differential entropy to reduce the uncertainty [41]. The ES acquisition function is formulated as follows:

$$U_{ES}(\mathbf{x}) = H(p(x^*|\mathcal{D})) - \mathbb{E}_{f(\mathbf{x})|\mathcal{D}}[H(p(x^*|f(\mathbf{x}), \mathcal{D}))] \quad (8)$$

where  $H(p(x^*))$  is the entropy of the posterior distribution at the current iteration on the location of the minimum of the objective function  $x^*$ , and  $\mathbb{E}_{f(\mathbf{x})}[\cdot]$  is the expectation over  $f(\mathbf{x})$  of the entropy of the posterior distribution at the next iteration on  $x^*$ . Typically, the exact calculation of the second term of Equation (8) is not possible and requires complex and expensive computational techniques to provide an approximation of  $U_{ES}(\mathbf{x})$ .

The Max-value entropy search (MES) [42] acquisition function is derived from the ES acquisition function and allows to reduce the computational effort required to estimate Equation (8) measuring the differential entropy of the minimum-value of the objective function:

$$U_{MES}(\mathbf{x}) = H(p(f|\mathcal{D})) - \mathbb{E}_{f(\mathbf{x})|\mathcal{D}}[H(p(f|f^*, \mathcal{D}))] \quad (9)$$

where the first and the second term are now computed on the minimum value of the objective function  $f^*$ . This permits to simplify the computations and to approximate the second term through a Monte Carlo strategy [42]. The analysis of the derivatives is not possible for the MES acquisition function since the formulation of the second term of Equation (9) is intractable.

As reported by Wang et al. [42] in their experimental analysis, MES targets the balance between the exploration of locations characterized by higher uncertainty of the surrogate model and the exploitation toward the believed minimum of the objective function. However, Nguyen et al. [100] demonstrate that MES might suffer from an imbalanced exploration/exploitation trade-off due to noisy observations of the objective function and to the discrepancy in the computation of the mutual information in the second term of Equation (9). As a result, MES might over-exploit the input space in presence of noise in measurements and over-explore when the discrepancy in the evaluation issue determines a pronounced sensitivity to the uncertainty of the surrogate model. Overall, the sampling scheme determined by the

MES acquisition function follows both the informativeness and representativeness/diversity learning criteria in active learning: the most promising sample is ideally selected targeting the balance between the increase of information about the objective function and the sampling toward the believed minimum predicted by the surrogate model.

### 3.3 Learning Criteria with Multiple Oracles

Active learning paradigms seek to maximize the capabilities of the learning process through the wise selection of the most informative samples to query at each iteration. However, most of the active learning strategies rely on a unique and omniscient source of information – also referred as oracle – to evaluate unknown samples, assuming that the associated prediction is exact. In many real world applications, multiple imperfect sources of information are available at different levels of reliability and cost, where usually increasing the accuracy of the prediction is associated with the increase of the cost of assessment. To address this realistic scenario, the active learning community proposes annotator-aware algorithms capable to include multiple oracles in the learning procedure, and select the optimal information source for each queried sample.

Active learning with multiple oracles shares the same learning criteria already presented for active learning with a single source of information (Section 3.1). However, the multiple information sources scenario determines an additional challenge in measuring the informativeness and representativeness/diversity of a specific location to query, since the sample can be evaluated with different degrees of accuracy and related computational cost. In this setting, the active learner selects the most promising sample with a trade-off between the reduction of uncertainty associated with reliable predictions and the cost required to acquire this prediction, to enhance the learning strategy while containing the total cost of the procedure. To further clarify the extension of the learning criteria adopted in active learning for the case of multiple oracles, the remaining of this section provides an overview of different methodologies representative of the multi-oracle learning criteria.

Several strategies for active learning with multiple oracles consider only the limited case of two sources of information, one of which is assumed to be omniscient while the other provides incorrect data with a certain fixed probability [101, 102, 103]. Typically, the extension to multiple sources of information is achieved through the relabeling approach, where samples are queried multiple times and the final query is obtained through majority voting [104]. Common techniques following this approach pursue the identification of a subset of oracles according to the proximity of their upper confidence bound to the maximum upper confidence bound, and apply the majority voting technique only considering the queries of this informative subset [105]. Other methods implement a repeating-labeling scheme where the algorithm integrates the repeated noisy prediction of the oracles to improve the quality of the labeling process, and the accuracy of the model learned from data [106]. The common drawback of voting-based schemes is that the same unknown sample is evaluated multiple times with different oracles, which results in a sub-optimal usage of the available sources of information. To overcome this limitations, several approaches rely on probabilistic models conceived for the multi-source scenario that allow to estimate the accuracy of each oracle in the prediction of unknown samples [107, 108], or using transfer knowledge approaches from unknown data in related domains to model the reliability of information sources [109]: these techniques enhance the simultaneous selection of the most informative location to sample and the associated most reliable source to query, increasing the performance of the active learning sampling procedure. Recent advancements in multiple oracles active learning are cost-effective algorithms, where the cost of an oracle is evaluated considering both the overall reliability of the prediction and the quality of labels in specific locations [110, 111, 112]. The cost-effectiveness property ensures that the selected location to sample allows to improve the accuracy of the predictive model and guarantees that the source of information to query provides an accurate prediction with a limited computational cost.

### 3.4 Multifidelity Acquisition Functions and Infill Criteria

This section further highlights the synergy between active learning and Bayesian optimization considering the availability of multiple sources of information that are leveraged to accomplish a specific learning goal. Similarly for the single information source frameworks, this symbiotic relationship is revealed through the common principles between the infill criteria adopted in multifidelity Bayesian optimization and the learning criteria implemented in active learning with multiple oracles. In the multifidelity scenario, the sampling procedure comes with an additional challenge: the decision making process involves not only the identification of promising samples but also the associated selection of the level of fidelity to query. This is reflected in the demand for infill criteria capable to define an efficient and balanced sampling policy through the multifidelity acquisition function, targeting the wise selection of samples to be evaluated with high-fidelity representations to contain the total computational cost required for the optimization procedure. Therefore, the multifidelity acquisition function  $U(x, l)$  specifies a policy to quantify the improvement of the solution that can be obtained evaluating a certain sample  $x$  with an associated level of fidelity  $l = 1, \dots, L$ .

Based on this considerations, the exploration and exploitation infill strategies are tailored according to the peculiarities of the multifidelity setting. The exploration defines a policy that incentivizes the adoption of low-fidelity evaluations to reduce the overall uncertainty of the multifidelity surrogate model while containing the demand for computational resources. The exploitation concentrates the sampling process in the regions of the search space where optimal solutions are likely to be located, emphasizing the use of high-fidelity evaluations to refine the solution of the optimization procedure. Multifidelity Bayesian optimization accentuates the dilemma between exploration and exploitation, since the library of information source characterized by different discrepancies in terms of accuracy and cost are available during the sampling procedure. This is reflected in the fact that the exploration process might benefit from high-fidelity data to reduce the uncertainty of the surrogate model in locations of the domain where the low-fidelity estimate is unreliable. Similarly, the exploitation procedure could leverage low-fidelity data to locally refine promising regions with a reduced computational expense, when the discrepancy between levels of fidelity is not pronounced.

The following sections are dedicated to the revision and discussion of popular formulations of the multifidelity acquisition function, namely the multifidelity expected improvement, multifidelity probability of improvement and multifidelity max-value entropy search. These formulations provide an overview of the principles driving the Bayesian sampling procedure in presence of multiple information sources, and highlight the equivalence between the multifidelity infill criteria and the multi-oracle learning criteria. This permits to identify the elements that underline the symbiotic relationship that exists between multifidelity Bayesian optimization and multi-oracle active learning.

### 3.4.1 Multifidelity Expected Improvement

The Multifidelity Expected Improvement (MFEI) relies on the EI acquisition function to define a sampling scheme in the multifidelity setting as follows [63]:

$$U_{MFEI}(\mathbf{x}, l) = U_{EI}(\mathbf{x}, L) \alpha_1(\mathbf{x}, l) \alpha_2(\mathbf{x}, l) \alpha_3(\mathbf{x}, l) \quad (10)$$

where  $U_{EI}(\mathbf{x}, L)$  is the expected improvement depicted in Equation (2) evaluated at the highest level of fidelity  $L$ , and the utility functions  $\alpha_1$ ,  $\alpha_2$  and  $\alpha_3$  are defined as follows:

$$\alpha_1(\mathbf{x}, l) = \text{corr} \left[ f^{(l)}, f^{(L)} \right] \quad (11)$$

$$\alpha_2(\mathbf{x}, l) = 1 - \frac{\sigma_\varepsilon}{\sqrt{\sigma^{2(l)}(\mathbf{x}) + \sigma_\varepsilon^2}} \quad (12)$$

$$\alpha_3(l) = \frac{\lambda^{(L)}}{\lambda^{(l)}}. \quad (13)$$

The first element  $\alpha_1$  is the posterior correlation coefficient between the level of fidelity  $l$  and the high-fidelity level  $L$ , and accounts for reduction of the expected improvement when a sample is evaluated with a low fidelity model. This term reflects a measure of the informativeness of the  $l$ -th source of information balancing the amount of improvement achievable evaluating a specific sample using the the high-fidelity level  $L$  with the reliability of the prediction associated with the level of fidelity  $l$ . The effect of  $\alpha_1$  is to modify the sampling scheme following the same principle of the informativeness criteria in active learning with multiple oracles by adding a penalty in the formulation that reduces the  $U_{MFEI}$  when  $1 \leq l < L$ , to include awareness about the increase of uncertainty associated with a low-fidelity prediction. The second element  $\alpha_2$  is conceived to adjust the expected improvement when the output at the  $l$ -th level of fidelity contains random errors. This is equivalent to consider the reduction of the uncertainty on the multifidelity Gaussian process prediction after a new evaluation of the objective function is added to the dataset  $\mathcal{D}$ . This function allows to improve the reliability of the  $U_{MFEI}$  when the representation of  $f^{(l)}$  at different levels of fidelity is affected by noise in the measurements. The third element  $\alpha_3$  is formulated as the ratio between the computational cost of the high-fidelity level  $L$  and the  $l$ -th level of fidelity, to balance the informative contributions of high- and a lower-fidelity observation and the related computational resources required for the evaluation. The effect of this term is to incentive the use of low-fidelity representations if almost the same expected improvement can be achieved with a high-fidelity evaluation.

### 3.4.2 Multifidelity Probability of Improvement

The Multifidelity Probability of Improvement (MFPI) acquisition function is the extension of the PI to a multifidelity scenario where multiple representations of  $f^{(l)}$  are available at different levels of fidelity [62]:

$$U_{MFPI}(\mathbf{x}, l) = U_{PI}(\mathbf{x}, L) \eta_1(\mathbf{x}, l) \eta_2(l) \eta_3(\mathbf{x}, l) \quad (14)$$

where the PI acquisition function (Equation (5)) is computed considering the highest-fidelity level  $L$  available, and the utility function  $\eta_1$ ,  $\eta_2$  and  $\eta_3$  are defined as follows:

$$\eta_1(\mathbf{x}, l) = \text{corr} [f^{(l)}, f^{(L)}] \quad (15)$$

$$\eta_2(l) = \frac{\lambda^{(L)}}{\lambda^{(l)}} \quad (16)$$

$$\eta_3(\mathbf{x}, l) = \prod_{i=1}^{n_l} [1 - R(\mathbf{x}, \mathbf{x}_i^{(l)})]. \quad (17)$$

The first term  $\eta_1$  is formulated as the  $\alpha_1$  utility function in Equation (11) and accounts for the increase of uncertainty associated with low-fidelity representations  $1 \leq l < L$ , if compared with the high-fidelity output  $L$ . This allows to reduce the probability of improvement if a low-fidelity representation is queried at a specific location of the input space. As already highlighted in Section 3.4.1,  $\eta_1$  realizes a form of informativeness learning making the most of the information sources at different levels of fidelity considering their reliability. This element produces the reduction of the computational cost associated with the over-exploitative nature of the PI (Section PI):  $\eta_1$  encourages the use of fast low-fidelity data, if the uncertainty of the  $l$ -th level of fidelity is not relevant in comparison with the high-fidelity  $L$ , reducing the number of high-fidelity calls during the exploitation of the domain. Similarly, the second function  $\eta_2$  shares the same formulation with the  $\alpha_3$  term in Equation (13), and balances the computational costs and the informative contributions related to the high-fidelity and lower-fidelity observations. The third element  $\eta_3$  is the sample density function and is computed as the product of the complement to unity of the spatial correlation function  $R(\cdot)$  [113] evaluated for the  $n_l$  samples considering the  $l$ -th level of fidelity. This term is conceived to reduce the acquisition function in locations already explored to prevent clustering of the sampling data as a result of the over-exploitative nature of the probability of improvement (Section 3.2.2).

### 3.4.3 Multifidelity Entropy Search and Multifidelity Max-Value Entropy Search

The Multifidelity Entropy Search (MFES) acquisition function is formulated extending the ES acquisition function to a multifidelity scenario [64]

$$U_{MFES}(\mathbf{x}) = H(p(x^*|\mathcal{D})) - \mathbb{E}_{f^{(l)}(\mathbf{x})|\mathcal{D}}[H(p(x^*|f^{(l)}(\mathbf{x}), \mathcal{D}))] \quad (18)$$

where the expectation term  $\mathbb{E}_{f^{(l)}(\mathbf{x})}[\cdot]$  considers multiple levels of fidelity  $l = 1, \dots, L$ . Similarly to the ES acquisition function, the computation of the expectation in Equation (18) is not possible in closed-form and requires an intensive procedure to provide a reliable approximation.

The Multifidelity Max-Value Entropy Search (MFMES) acquisition function can be formulated extending the max-value entropy search to a multifidelity setting as follows [65]:

$$U_{MFMES}(\mathbf{x}) = [H(p(f^{(l)}|\mathcal{D})) - \mathbb{E}_{f^{(l)}(\mathbf{x})|\mathcal{D}}[H(p(f^{(l)}|f^{*L}, \mathcal{D}))]] / \lambda^{(l)} \quad (19)$$

where the differential entropy is measured on the minimum value of the objective function  $f^{*L}$  considering the high-fidelity representation  $L$ . In this case, the approximation of the expectation term in Equation (19) relies on a Monte Carlo strategy that allows to contain the computational cost if compared with the procedure used for the MFES acquisition function [65].

In the multifidelity scenario, the MFMES acquisition function measures the information gain obtained evaluating the objective function  $f^{(l)}(\mathbf{x})$  at certain location  $\mathbf{x}$  and associated level of fidelity  $l$  with respect to the global minimum of the objective function. This can be interpreted as the reduction in the uncertainty of the minimum value  $f^{*L}$  by observing  $f^{(l)}(\mathbf{x})$ , where this uncertainty is measured as the differential entropy associated with the  $l$ -th level of fidelity. The computational cost  $\lambda^{(l)}$  of the  $l$ -th level of fidelity is introduced in Equation (19) to balance the increase of uncertainty that characterizes lower levels of fidelity with the reduction of the computational resources required for the query. As already discussed in Section 3.2.3 for the max-value entropy search, also the multifidelity differential entropy in Equation (19) allows to balance the informativeness and the representativeness/diversity acquired evaluating a certain sample with an associated level of fidelity.

## 4 Experiments

In the following section, we illustrate and discuss the comparison between the acquisition functions for both single-fidelity and multifidelity Bayesian optimization over a set of benchmark problems conceived to stress the algorithms highlighting advantages and weaknesses of the different learning criteria in presence of challenging mathematical properties of the objective function [26]. For this comparative study, we consider the expected improvement (Section 3.2.1), probability of improvement (PI) (Section 3.2.2), and Max-Value Entropy Search (MES) (Section 3.2.3) for the single-fidelity frameworks and their multifidelity counterparts Multifidelity Expected Improvement (MFEI) (Section 3.4.1), Multifidelity Probability of Improvement (MFPI) (Section 3.4.2) and Multifidelity Max-Value Entropy Search (FMES) (Section 3.4.3).

We impose the same initial condition for both the single-fidelity and multifidelity algorithms. The initial setting include: (i) the number of samples  $N_0^{(l)}$  for each level of fidelity  $l$  that defines the initial dataset to compute the first surrogate model of the objective function, (ii) the computational cost assigned to each level of fidelity  $\lambda^{(l)}$ , and (iii) the maximum computational budget  $B_{max}$  allocated for each benchmark problem defined linearly with the dimensionality  $D$  of the problem  $B_{max} = 100D$ , where the budget  $B = \sum \lambda_i^{(l)}$  and measured as the cumulative computational cost expended during the optimization at each iteration  $i$ . The initial dataset  $N_0^{(l)}$  is obtained through Latin hypercube sampling for all the numerical experiments [114] to ensure the full coverage of the range of the optimization variables. All the methods are based on the Gaussian processes surrogate model and its extension to the multifidelity setting. We implement the square exponential kernels for all the GP covariances, and use the maximum likelihood estimation approach to optimize the hyperparameters of the kernel and the mean function of the GP [115].

### 4.1 Benchmark Problems

The set of benchmark problems implemented in this comparative study includes the Forrester function continuous and discontinuous, the Rosenbrock function, the Rastrigin function shifted and rotated, the ALOS functions, a coupled spring-mass optimization problem and the noisy Paciorek function. This specific set of functions allows to exemplify mathematical properties and behaviors that also characterize real-world optimization problems without increasing the complexity and computational onerousness required for their evaluation.

#### 4.1.1 Forrester Function

The Forrester function is a one-dimensional non linear function over the domain  $[0,1]$  that allows to capture the overall behaviour of optimization algorithms. For this benchmark problem, four levels of fidelity are available:

$$f^{(4)}(\mathbf{x}) = (6\mathbf{x} - 2)^2 \sin(12\mathbf{x} - 4) \quad (20)$$

$$f^{(3)}(\mathbf{x}) = (5.5\mathbf{x} - 2.5)^2 \sin(12\mathbf{x} - 4) \quad (21)$$

$$f^{(2)}(\mathbf{x}) = 0.75f_1(\mathbf{x}) + 5(\mathbf{x} - 0.5) - 2 \quad (22)$$

$$f^{(1)}(\mathbf{x}) = 0.5f_1(\mathbf{x}) + 10(\mathbf{x} - 0.5) - 5. \quad (23)$$

where  $f^{(4)}$  is the high-fidelity function and the levels of fidelity  $l = 1, 2, 3, 4$  increase with the accuracy of the representations. The analytical minimum of the Forrester function is equal to  $f^{*(4)} = -6.0207$  and is located at the input point  $x^* = 0.7572$ .

#### 4.1.2 Discontinuous Forrester Function

The Discontinuous Forrester function benchmark introduces a discontinuity in the formulation of the standard Forrester function to analyse the behaviour of optimization algorithms in presence of objective functions non continuous over the input space. We consider two levels of fidelity as follows:

$$f^{(2)}(\mathbf{x}) = \begin{cases} (6\mathbf{x} - 2)^2 \sin(12\mathbf{x} - 4), & 0 \leq \mathbf{x} \leq 0.5 \\ (6\mathbf{x} - 2)^2 \sin(12\mathbf{x} - 4) + 10, & 0.5 < \mathbf{x} \leq 1 \end{cases} \quad (24)$$

$$f^{(1)}(\mathbf{x}) = \begin{cases} 0.5f^{(2)}(\mathbf{x}) + 10(\mathbf{x} - 0.5) - 5, & 0 \leq \mathbf{x} \leq 0.5 \\ 0.5f^{(2)}(\mathbf{x}) + 10(\mathbf{x} - 0.5) - 2 & 0.5 < \mathbf{x} \leq 1 \end{cases} \quad (25)$$

where  $f^{(2)}$  is the high-fidelity representation. The optimum is located at  $x^* = 0.75724876$  corresponding to a value of the objective equal to  $f^{*(2)} = -0.9863$ .

#### 4.1.3 Rosenbrock Function

The Rosenbrock function is a well accepted non-convex problem for testing optimization methods, and is defined in  $\chi = [-2, 2]^D$  where  $D$  is the dimensionality of the input space. We implemented three levels of fidelity formulated as follows:

$$f^{(3)}(\mathbf{x}) = \sum_{i=1}^{D-1} 100(\mathbf{x}_{i+1} - \mathbf{x}_i^2)^2 + (1 - \mathbf{x}_i)^2 \quad (26)$$

$$f^{(2)}(\mathbf{x}) = \sum_{i=1}^{D-1} 50(\mathbf{x}_{i+1} - \mathbf{x}_i^2)^2 + (-2 - \mathbf{x}_i)^2 - \sum_{i=1}^D 0.5\mathbf{x}_i \quad (27)$$

$$f^{(1)}(\mathbf{x}) = \frac{f^{(3)}(\mathbf{x}) - 4 - \sum_{i=1}^D 0.5\mathbf{x}_i}{10 + \sum_{i=1}^D 0.25\mathbf{x}_i} \quad (28)$$

where the high-fidelity function is  $f^{(3)}$  and the lower-fidelities are obtained using a transformation of  $f^{(3)}$  based on linear additive and multiplicative factors [116]. The analytical minimum is located at  $x^* = [1, 1]^D$  and corresponds to a value of the objective function  $f^{*(3)} = 0$ . The scalability of the Rosenbrock function with  $D$  of the formulation allows to test the performance of the methods at increasing dimensionality of the input space. For the purposes of this study, we consider the cases  $D = 2, 5, 10$ .

#### 4.1.4 Shifted-Rotated Rastrigin Function

The Rastrigin function is commonly used as test function to represent real-world applications where the objective function might present an high multimodal behaviour. We adopt a benchmark problem based on the original formulation of the Rastrigin function shifted and rotated as follows:

$$f(\mathbf{z}) = \sum_{i=1}^D (z_i^2 + 1 - \cos(10\pi z_i)), \quad (29)$$

where:  $\mathbf{z} = R(\theta)(\mathbf{x} - \mathbf{x}^*)$  and  $R(\theta) = \begin{bmatrix} \cos \theta & -\sin \theta \\ \sin \theta & \cos \theta \end{bmatrix}$  is the rotation matrix with the rotation angle fixed at  $\theta = 0.2$ . We define three levels of fidelity for this benchmark problems as follows [117]:

$$f^{(l)}(\mathbf{z}, \phi) = f(\mathbf{z}) + e_r(\mathbf{z}, \phi_i) \quad (30)$$

where  $e_r(\mathbf{z}, \phi_i)$  is the resolution error:

$$e_r(\mathbf{z}, \phi) = \sum_{i=1}^2 a(\phi) \cos^2(w(\phi)z_i + b(\phi) + \pi). \quad (31)$$

with  $\Theta(\phi) = 1 - 0.0001\phi$ ,  $a(\phi) = \Theta(\phi)$ ,  $w(\phi) = 10\pi\Theta(\phi)$ , and  $b(\phi) = 0.5\pi\Theta(\phi)$ . Thus, we define the high-fidelity function  $f^{(3)}(\phi = 10000)$ , the intermediate fidelity function  $f^{(2)}(\phi = 5000)$  and the low-fidelity function  $f^{(1)}(\phi = 2500)$ . For this benchmark, the input variables are defined within the interval  $\chi = [-0.1, 0.2]^2$  and the analytical optimum is  $f^{*(3)} = 0$  located at  $x^* = [0.1, 0.1]$ .

#### 4.1.5 ALOS Functions

The Agglomeration of Locally Optimized Surrogate (ALOS) functions [118] are conceived to emulate real-world applications where the objective functions is characterized by oscillatory phenomena at different frequency distributed along the domain. This is a heterogeneous and non-polynomial function defined on unit hypercubes up to three

dimensions useful to assess the goodness of the surrogate model in presence of localized behaviours. For the ALOS benchmark, we consider two levels of fidelity and increasing dimensionality of the input space  $D = 1, 2, 3$ :

$$\begin{cases} f^{(2)}(\mathbf{x}) &= \sin[30(\mathbf{x} - 0.9)^4] \cos[2(\mathbf{x} - 0.9)] + (\mathbf{x} - 0.9)/2 \\ f^{(1)}(\mathbf{x}) &= (f^{(2)}(\mathbf{x}) - 1.0 + \mathbf{x}) / (1.0 + 0.25\mathbf{x}) \end{cases} \quad \text{for } D = 1 \quad (32)$$

$$\begin{cases} f^{(2)}(\mathbf{x}) &= \sin[21(\mathbf{x}_1 - 0.9)^4] \cos[2(\mathbf{x}_1 - 0.9)] + (\mathbf{x}_1 - 0.7)/2 + \sum_{i=2}^D i\mathbf{x}_i \sin\left(\prod_{j=1}^i \mathbf{x}_j\right) \\ f^{(1)}(\mathbf{x}) &= (f^{(2)}(\mathbf{x}) - 2.0 + \sum_{i=1}^D \mathbf{x}_i) / (5.0 + \sum_{i=1}^2 0.25i\mathbf{x}_i - \sum_{i=3}^D 0.25i\mathbf{x}_i). \end{cases} \quad \text{for } D \geq 2. \quad (33)$$

For  $D = 1$ , the analytical optimum is located at  $x^* = 0.2755$  corresponding to  $f^{*(2)} = -0.6250$  while for  $D \geq 2$  the minimum is located at  $x^* = [0, 0]^D$  with value of the objective function  $f^{*(2)} = -0.5627123$

#### 4.1.6 Spring-Mass System

This benchmark problem consists of a coupled spring mass system composed of two masses connected by two springs. We consider the masses  $m_1$  and  $m_2$  concentrated at their center of gravity and the elastic behaviour of the two spring modeled through the Hooke's law and characterized by the Hooke's constants  $k_1$  and  $k_2$ , respectively. Considering a friction-less dynamics, it is possible to define the equations of motion as follows

$$m_1 \ddot{h}_1(t) = (-k_1 - k_2)h_1(t) + k_2 h_2(t) \quad (34)$$

$$m_2 \ddot{h}_2(t) = k_2 h_1(t) + (-k_1 - k_2)h_2(t). \quad (35)$$

where  $h_1(t)$  and  $h_2(t)$  are the positions of the masses as a function of time  $t$ .

Equation (34) can be solved using the fourth-order accurate Runge-Kutta time-marching method and varying the time-step  $dt$  to define two fidelity levels. Specifically, we define the high-fidelity model  $f^{(2)}(dt = 0.01)$  and the low-fidelity model  $f^{(1)}(dt = 0.6)$ . The benchmark problem consists in the identification of the combination of masses and Hooke's constants of spring  $\mathbf{x} = [m_1, m_2, k_1, k_2]$  that minimizes  $h_1(t = 6)$  considering the input space  $\chi = [1, 4]^4$  and the initial conditions of motion  $h_1 = h_2 = 0$  and  $\dot{h}_1 = \dot{h}_2 = 0$ .

#### 4.1.7 Paciorek Function with Noise

The Paciorek function [119] is characterized by a localized and multimodal behaviour that makes challenging the solution of the optimization task. We introduce in the formulation a uniformly distributed random noise term to investigate the performance of the algorithms in presence of noisy observations of the objective function. The benchmark problem consists of two levels of fidelity defined as follows:

$$f^{(2)}(\mathbf{x}) = \sin\left(\prod_{i=1}^D \mathbf{x}_i\right)^{-1} + \text{rand.normal}(0, \alpha_1) \quad (36)$$

$$f^{(1)}(\mathbf{x}) = f^{(2)}(\mathbf{x}) - 9A^2 \cos\left(\prod_{i=1}^D \mathbf{x}_i\right)^{-1} + \text{rand.normal}(0, \alpha_2) \quad (37)$$

where  $A = 0.5$ ,  $\alpha_1 = 0.0125$ ,  $\alpha_2 = 0.075$ , and the input variable is defined across the input domain  $\chi = [0, 3, 1]^2$ .

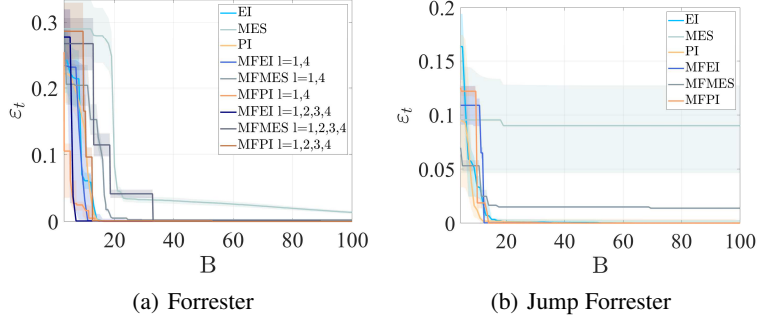


Figure 1: Performances of the competing algorithms for the Forrester and Jump Forrester benchmarks.

## 4.2 Results

In the following, we illustrate and discuss the results obtained with both single fidelity (Section 3.2) and multifidelity (Section 3.4) Bayesian optimization algorithms. We define the following evaluation metrics to assess the performances of the algorithms [26]:

$$\epsilon_x \equiv \frac{\|\mathbf{x}^* - \hat{\mathbf{x}}^*\|}{\sqrt{N}}, \quad (38)$$

$$\epsilon_f \equiv \frac{f(\hat{\mathbf{x}}^*) - f^*}{f_{max} - f^*}, \quad (39)$$

$$\epsilon_t \equiv \sqrt{\frac{\epsilon_x^2 + \epsilon_f^2}{2}} \quad (40)$$

where  $\mathbf{x}^*$  is the location of the analytical optimum,  $\hat{\mathbf{x}}^*$  is the optimum identified by the algorithm, and  $f_{max}$  and  $f^*$  are the maximum and minimum of the objective function, respectively. Specifically,  $\epsilon_x$  represents the normalized error in the search space,  $\epsilon_f$  evaluates the error related to the objective function and  $\epsilon_t$  allows to assess both the design and goal accuracy [120].

We evaluate the metric  $\epsilon_t$  as a function of the computational budget  $B$  defined as the cumulative computational cost associated with observations of the objective function at the  $l$ -th level of fidelity. We run 10 trails for each benchmark problem presented in Section 4.1 to compensate the influence of the random initial design of experiments, and to verify the sensitivity and robustness of the algorithms to the initial sampling. The results are reported in terms of median values of  $\epsilon_t$  together with the values falling in the interval between the 25-th and 75-th percentiles.

Figure 1 summarizes the outcome obtained for the Forrester function and Discontinuous Forrester Function. The results for the Forrester benchmark (Figure 1(a)) show that the multifidelity algorithms permit to identify the optimum solution with a significant reduction of the computational budget if compared with the single fidelity counterparts. The best performing algorithm is the MFEI considering the complete benchmark with all the levels of fidelity available  $l = 1, 2, 3, 4$  while the second best is the MFEI implementing only the high-fidelity  $l = 4$  and the lower-fidelity  $l = 1$ . These outcomes suggest that the balance between exploration and exploitation provided by the MFEI and EI algorithms improves the performance of the optimization process: the MFEI strategy outperforms the MFPI and MFMES, while the PI algorithm shows better results in terms of reduction of  $\epsilon_t$  if compared with EI and MES.

The EI shows a slow reduction of  $\epsilon_t$  in the first phase of the optimization process, and then a fast convergence toward the analytical optimum. This is the result of the balance between exploration and exploitation: the learner uses the first samples to improve the information about the objective function over the input space, and afterwards refines the solution of the optimization exploiting the region where it is believed that the optimum is located. The PI algorithm exhibits an over-exploitation of the input space characterized by a significant decrease of  $\epsilon_t$  and the rapid assessment the optimum. This result can be explained with the low-dimension of the input space ( $D = 1$ ): a relatively low number of observations of the objective function are required to compute an accurate surrogate model improving the learning process toward the optimum. Conversely, the MES shows an over-exploratory sampling process that fails in the identification of the optimum since all the computational resources are employed for the massive exploration of the input space rather than concentrate the samples closer to the believed optimum.

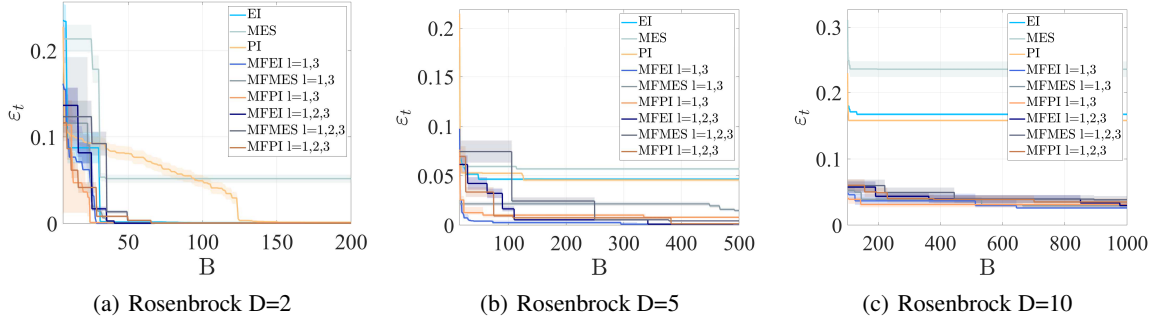


Figure 2: Performances of the competing algorithms for the Rosenbrock benchmarks.

Considering the outcomes of the multifidelity algorithms, the MFEI improves the performance of optimization leveraging low-fidelity data to reduce the computational cost of exploration, and using a limited number of high-fidelity data to exploit the domain to reduce the budget required to assess the optimum. This can be noticed with the reduction of the budget used for the first exploration phase with a slow decrease of  $\varepsilon_t$ , and the successive identification of the optimum with a contained budget expenditure. The MFEI algorithm accentuates this behaviour when all the levels of fidelity are considered using wisely the intermediate levels of fidelity  $l = 2, 3$  to further decrease the cost for the identification of the analytical optimum. The MFPI reduces the over-exploitation that characterizes the PI using at best the low-fidelity data to reduce the computational cost for optimization. Specifically, the complete case  $l = 1, 2, 3, 4$  presents an exploration phase similar to the MFEI search before the exploitation toward the optimum, proving a balanced learning process between informativeness and representativeness/diversity. The FMES leverages the multiple information sources at different levels of fidelity improving the capabilities of MES algorithm in the identification of the analytical optimum. However, the FMES is not capable to take advantage from all the four representations  $l = 1, 2, 3, 4$  leading to a suboptimal performance if compared with the FMES implementing only  $l = 1, 4$ . This outcome can be justified with a massive exploration phase that uses all the sources of information without an effective balance between cost and accuracy.

The outcomes on the discontinuous Forrester function (Figure 1(b)) show the same behaviours of the continuous Forrester: the multifidelity algorithms outperform the single fidelity counterpart thanks to the availability of multiple representations of the objective function. Specifically, the MFEI takes full advantage of the low-fidelity data to learn the discontinuity and assess the optimum solution, demonstrating the importance of the balance between accuracy and cost during the learning process. It should be noted that both the MES and FMES identify a suboptimal solution of the optimization problem due to an expensive exploration phase where the median value of  $\varepsilon_t$  remains constant with the budget  $B$ .

Figure 2 illustrates the experiments on the Rosenbrock function conducted increasing the dimensionality of the domain  $D$  to investigate how the performances of the competing algorithms evolve with the number of variables. The multifidelity methods successfully improve the performance of optimization if compared with the single-fidelity counterparts. Specifically, the MFEI algorithm outperforms the competing methods for all the dimensions of the input space considered in this study. For  $D = 2$  (Figure 2(a)), the MFEI implementing two levels of fidelity  $l = 1, 3$  identifies the analytical optimum after an exploration phase that involves mostly low-fidelity queries to contain the total computational cost, while the MFEI implementing the complete set of levels of fidelity  $l = 1, 2, 3$  is not capable to make advantage of the intermediate fidelity  $l = 2$  during the exploration phase increasing its computational cost. It should be noticed that the FMES is capable to converge to the analytical optimum considering both the case implementing  $l = 1, 3$  and  $l = 1, 2, 3$  thanks to the low-fidelity data that reduces the computational cost required for the exploration. Increasing the dimension of the input space to  $D = 5$  (Figure 2(b)), the multifidelity algorithms successfully assess the optimum solution while the single-fidelity algorithms fail in the identification task with the allocated budget. This performance reflects the decrease of the accuracy of the Gaussian process with dimensionality: the single-fidelity methods tend to explore the input space to improve the reliability of the surrogate model without a pronounced phase of exploitation toward the optimum. In contrast, the multifidelity algorithms leverage low-fidelity data during the exploration phase improving the accuracy of the multifidelity Gaussian process with a relatively low computational cost. At  $D = 10$  (Figure 2(c)), all the algorithms are not capable to reach the analytical optimum with the allocated budget due to the unreliable prediction of the Gaussian process that requires a significant number of evaluations to reduce the uncertainty of the prediction.

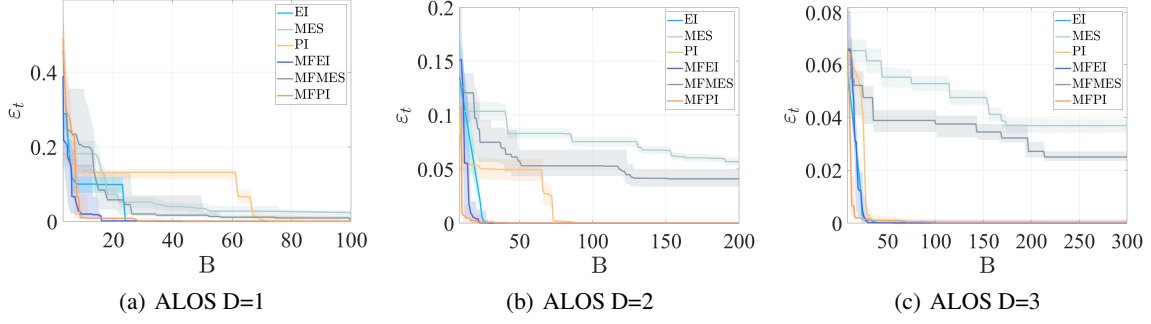


Figure 3: Performances of the competing algorithms for the ALOS benchmarks.

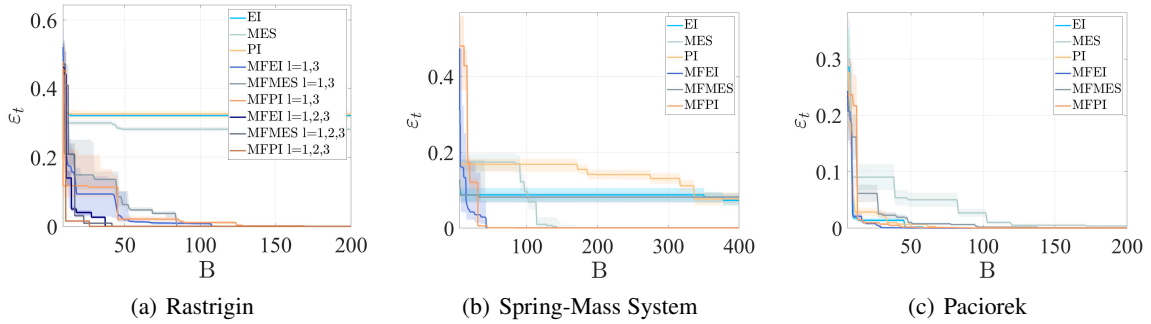


Figure 4: Performances of the competing algorithms for the multimodal benchmarks.

The results obtained for the ALOS benchmark problem in Figure 3 illustrate that the MFEI outperforms all the competing methods achieving a significant reduction of  $\epsilon_t$  with a limited computational cost for the one- (Figure 3(a)), two- (Figure 3(b)) and three- (Figure 3(c)) dimensional problem. It is important to emphasize that the second best performing algorithm is the single-fidelity EI that outperforms the other multifidelity and single-fidelity algorithms (MFEI, MFMES, PI, MES). This result can be explained with the capability of the MFEI and EI algorithms to identify the most informative samples that allow to improve the accuracy of the surrogate model thanks to the balance between the informativeness of unknown locations and their representativeness. Moreover, the MFEI achieves better optimization performances, thanks to the use of low-fidelity data to contain the total computational cost required to assess the optimum. The results suggest that the trade-off between exploration and exploitation allows to enhance the optimization performance in presence of objective functions characterized by oscillations at different frequencies.

The outcomes related to the multimodal benchmarks are reported in Figure 4. The multifidelity algorithms are capable to converge toward the analytical optimum with a fraction of the computational cost, if compared with the the single-fidelity results. For the Rastrigin function (Figure 4(a)), the multifidelity methods implementing all the levels of fidelity  $l = 1, 2, 3$  outperforms the multifidelity methods with  $l = 1, 3$ : the intermediate level of fidelity  $l = 2$  is more accurate, if compared with the low-fidelity output  $l = 3$  and allows to improve the reliability of the Gaussian process in presence of a strong multimodal behaviour. The best performing method is MFPI using  $l = 1, 2, 3$  denoting that the over-exploitation of the input space with lower-fidelities levels  $l = 2, 3$  allows to take full advantage from low-fidelity data, improving the performance of the learning process. The results for the mass spring benchmark problem (Figure 4(b)) confirm the superior convergence to the optimum of the multifidelity methods. However, we observed that the MES algorithm is capable to identify the optimum while the MFMES converges to a sub-optimal solution. This undesirable performance is related to the already noticed over-exploratory behaviour: the MES uses high-fidelity data  $l = 1$  to explore the input space refining the accuracy of the surrogate model, while the MFMES uses only low-fidelity data for exploration without querying the high-fidelity model to contain the computational cost. Considering the outcomes for the Paciorek function (Figure 4(c)), the MFEI outperforms the competing method reducing  $\epsilon_t$  to zero with a fraction of the computational cost while the EI shows better convergence to the optimum if compared with PI and MES. These outcomes suggest that the balance between exploration and exploitation is essential in presence of local multimodal behaviour and noise in the measurements of the objective function. It should be noticed that in presence of noise both

the MES and MFMES show an attenuation of the exploratory behaviour and a greater exploitation of the domain. This result is in agreement with what observed by Nguyen et al. [100].

The results obtained for all the benchmark problems reveal that the MFEI and the EI strategies lead to overall better performances for multifidelity and single-fidelity optimization, respectively, if compared with the other competing methods. This demonstrates that the balance between the exploration of the domain and exploitation toward the optimum is essential to improve the accuracy of the surrogate model with a contained computational budget, and take advantage from the acquired data to rapidly identify the optimum. Moreover, we noticed that the pure exploitation might be useful for low-dimensional problems where a limited number of data are sufficient to compute an accurate surrogate model, while the pure exploration might be convenient for large dimensionality of the domain where a significant number of observations are required to improve the reliability of the surrogate model.

## 5 Concluding Remarks

This position paper proposes an original unified perspective that exhibits the symbiotic relationship between Bayesian optimization and active learning as adaptive sampling frameworks to achieve a certain learning goal. Particular attention is dedicated to this synergy for the case of learning schemes based on a single source of information – Bayesian optimization and active learning –, and when multiple sources at different levels of fidelity are available – multifidelity Bayesian optimization and multiple oracles active learning. This interpretation is based on the dualism between the learning criteria that drive the sampling procedure in active learning, and the infill criteria realized through the acquisition function that permits to evaluate promising locations of the search domain. Our arguments are guided by an overview of Bayesian optimization frameworks and active learning paradigms, with emphasis on pool-based active learning as the methodology that shows the closest analogy to the Bayesian scheme. To support our position, we identify the key learning criteria that characterize the pool-based active learning framework, namely the informativeness and representativeness/diversity of samples to be evaluated, and we highlight the substantial dualism in principle with the Bayesian infill criteria of exploration and exploitation. In addition, we emphasize that this synergy exists even when multiple information sources are available, weaving a parallelism between the learning criteria in multiple oracles active learning and the infill criteria in multifidelity Bayesian optimization. This is formalized and demonstrated through the review and discussion of popular acquisition functions for Bayesian optimization and their formulation extended to the multifidelity scenario, emphasizing how Bayesian infill criteria realize an adaptive sampling scheme pursuing a learning goal in ways substantially equal to the learning criteria in active learning. Using analytical benchmark problems, we demonstrate the benefits of each learning/infill criteria over stressfull mathematical properties of the objective function that characterize real-world applications, such as discontinuities, local and global multimodality, varying frequency of oscillation and noise. The results demonstrate the importance of balancing exploration and exploitation to improve the accuracy of solutions and the computational efficiency.

## References

- [1] Timothy W Simpson, Jesse D Poplinski, Patrick N Koch, and Janet K Allen. Metamodels for computer-based engineering design: survey and recommendations. *Engineering with computers*, 17:129–150, 2001.
- [2] Felipe AC Viana, Christian Gogu, and Raphael T Haftka. Making the most out of surrogate models: tricks of the trade. In *International design engineering technical conferences and computers and information in engineering conference*, volume 44090, pages 587–598, 2010.
- [3] Timothy Simpson, Vasilli Toropov, Vladimir Balabanov, and Felipe Viana. Design and analysis of computer experiments in multidisciplinary design optimization: a review of how far we have come-or not. In *12th AIAA/ISSMO multidisciplinary analysis and optimization conference*, page 5802, 2008.
- [4] Nestor V Queipo, Raphael T Haftka, Wei Shyy, Tushar Goel, Rajkumar Vaidyanathan, and P Kevin Tucker. Surrogate-based analysis and optimization. *Progress in aerospace sciences*, 41(1):1–28, 2005.
- [5] Gary Wang and S. Shan. Review of metamodeling techniques in support of engineering design optimization. *Journal of Mechanical Design - J MECH DESIGN*, 129, 04 2007.
- [6] Raphael T Haftka, Diane Villanueva, and Anirban Chaudhuri. Parallel surrogate-assisted global optimization with expensive functions—a survey. *Structural and Multidisciplinary Optimization*, 54:3–13, 2016.
- [7] Ke-Shi Zhang, Zhong-Hua Han, Zhong-Jian Gao, and Yuan Wang. Constraint aggregation for large number of constraints in wing surrogate-based optimization. *Structural and Multidisciplinary Optimization*, 59:421–438, 2019.
- [8] Dahua Du, Erming He, Feng Li, and Daoqiong Huang. Using the hierarchical kriging model to optimize the structural dynamics of rocket engines. *Aerospace Science and Technology*, 107:106248, 2020.

- [9] César Ramírez-Márquez, Edgar Martín-Hernández, Mariano Martín, and Juan Gabriel Segovia-Hernández. Surrogate based optimization of a process of polycrystalline silicon production. *Computers & Chemical Engineering*, 140:106870, 2020.
- [10] Truong Dang, Anh Vu Luong, Alan Wee Chung Liew, John McCall, and Tien Thanh Nguyen. Ensemble of deep learning models with surrogate-based optimization for medical image segmentation. In *2022 IEEE Congress on Evolutionary Computation (CEC)*, pages 1–8. IEEE, 2022.
- [11] Halil Beglerovic, Michael Stolz, and Martin Horn. Testing of autonomous vehicles using surrogate models and stochastic optimization. In *2017 IEEE 20th International Conference on Intelligent Transportation Systems (ITSC)*, pages 1–6. IEEE, 2017.
- [12] Amin Nazemian and Parviz Ghadimi. Multi-objective optimization of trimaran sidehull arrangement via surrogate-based approach for reducing resistance and improving the seakeeping performance. *Proceedings of the institution of mechanical engineers, part M: journal of engineering for the maritime environment*, 235(4):944–956, 2021.
- [13] Foster Provost, David Jensen, and Tim Oates. Efficient progressive sampling. In *Proceedings of the fifth ACM SIGKDD international conference on Knowledge discovery and data mining*, pages 23–32, 1999.
- [14] Felipe AC Viana, Timothy W Simpson, Vladimir Balabanov, and Vasilli Toropov. Special section on multidisciplinary design optimization: metamodeling in multidisciplinary design optimization: how far have we really come? *AIAA journal*, 52(4):670–690, 2014.
- [15] Haitao Liu, Yew-Soon Ong, and Jianfei Cai. A survey of adaptive sampling for global metamodeling in support of simulation-based complex engineering design. *Structural and Multidisciplinary Optimization*, 57:393–416, 2018.
- [16] Lisia Dias, Atharv Bhosekar, and Mariathi Ierapetritou. Adaptive sampling approaches for surrogate-based optimization. In *Computer Aided Chemical Engineering*, volume 47, pages 377–384. Elsevier, 2019.
- [17] Bobak Shahriari, Kevin Swersky, Ziyu Wang, Ryan P Adams, and Nando De Freitas. Taking the human out of the loop: A review of bayesian optimization. *Proceedings of the IEEE*, 104(1):148–175, 2015.
- [18] Peter I Frazier. A tutorial on bayesian optimization. *arXiv preprint arXiv:1807.02811*, 2018.
- [19] Harold J Kushner. A new method of locating the maximum point of an arbitrary multipeak curve in the presence of noise. 1964.
- [20] AG Zhilinskias. Single-step bayesian search method for an extremum of functions of a single variable. *Cybernetics*, 11(1):160–166, 1975.
- [21] Jonas Močkus. On bayesian methods for seeking the extremum. In *Optimization Techniques IFIP Technical Conference: Novosibirsk, July 1–7, 1974*, pages 400–404. Springer, 1975.
- [22] Donald R Jones, Matthias Schonlau, and William J Welch. Efficient global optimization of expensive black-box functions. *Journal of Global optimization*, 13(4):455–492, 1998.
- [23] Burr Settles. Active learning literature survey. 2009.
- [24] Liu Yang, Steve Hanneke, and Jaime Carbonell. A theory of transfer learning with applications to active learning. *Machine learning*, 90(2):161–189, 2013.
- [25] David D Lewis. A sequential algorithm for training text classifiers: Corrigendum and additional data. In *Acm Sigir Forum*, volume 29, pages 13–19. ACM New York, NY, USA, 1995.
- [26] L Mainini, A Serani, MP Rumpfkeil, E Minisci, D Quagliarella, H Pehlivan, S Yildiz, S Ficini, R Pellegrini, F Di Fiore, et al. Analytical benchmark problems for multifidelity optimization methods. *arXiv preprint arXiv:2204.07867*, 2022.
- [27] Bruce E Stuckman. A global search method for optimizing nonlinear systems. *IEEE Transactions on Systems, Man, and Cybernetics*, 18(6):965–977, 1988.
- [28] John F Elder. Global r/sup d/optimization when probes are expensive: the grope algorithm. In *[Proceedings] 1992 IEEE International Conference on Systems, Man, and Cybernetics*, pages 577–582. IEEE, 1992.
- [29] Rémi Lam, Matthias Poloczek, Peter Frazier, and Karen E Willcox. Advances in bayesian optimization with applications in aerospace engineering. In *2018 AIAA Non-Deterministic Approaches Conference*, page 1656, 2018.
- [30] Thomas A Zang. *Needs and opportunities for uncertainty-based multidisciplinary design methods for aerospace vehicles*. National Aeronautics and Space Administration, Langley Research Center, 2002.

- [31] Anthony T Patera. Shape optimization by bayesian-validated computer-simulation surrogates. Technical report, 1997.
- [32] R Michael Lewis and Luc Huyse. Aerodynamic shape optimization of two-dimensional airfoils under uncertain conditions. Technical report, Institute for Computer Applications in Science and Engineering Hampton Va, 2001.
- [33] Rémi Lam, Matthias Poloczek, Peter Frazier, and Karen E Willcox. Advances in bayesian optimization with applications in aerospace engineering. In *2018 AIAA Non-Deterministic Approaches Conference*, page 1656, 2018.
- [34] Ryan-Rhys Griffiths and José Miguel Hernández-Lobato. Constrained bayesian optimization for automatic chemical design using variational autoencoders. *Chemical science*, 11(2):577–586, 2020.
- [35] Peter I Frazier and Jialei Wang. Bayesian optimization for materials design. *Information science for materials discovery and design*, pages 45–75, 2016.
- [36] Huifang Kong, Jiapeng Yan, Hai Wang, and Lei Fan. Energy management strategy for electric vehicles based on deep q-learning using bayesian optimization. *Neural Computing and Applications*, 32:14431–14445, 2020.
- [37] Felix Berkenkamp, Andreas Krause, and Angela P Schoellig. Bayesian optimization with safety constraints: safe and automatic parameter tuning in robotics. *Machine Learning*, pages 1–35, 2021.
- [38] Carl Edward Rasmussen. Gaussian processes in machine learning. In *Summer school on machine learning*, pages 63–71. Springer, 2003.
- [39] Michael A Osborne, Roman Garnett, and Stephen J Roberts. Gaussian processes for global optimization. In *3rd international conference on learning and intelligent optimization (LION3)*, pages 1–15. Citeseer, 2009.
- [40] Harold J Kushner. A new method of locating the maximum point of an arbitrary multipeak curve in the presence of noise. 1964.
- [41] Philipp Hennig and Christian J Schuler. Entropy search for information-efficient global optimization. *Journal of Machine Learning Research*, 13(6), 2012.
- [42] Zi Wang and Stefanie Jegelka. Max-value entropy search for efficient bayesian optimization. In *International Conference on Machine Learning*, pages 3627–3635. PMLR, 2017.
- [43] Warren Scott, Peter Frazier, and Warren Powell. The correlated knowledge gradient for simulation optimization of continuous parameters using gaussian process regression. *SIAM Journal on Optimization*, 21(3):996–1026, 2011.
- [44] Remi Lam and Karen Willcox. Lookahead bayesian optimization with inequality constraints. *Advances in Neural Information Processing Systems*, 30, 2017.
- [45] Jian Wu and Peter Frazier. Practical two-step lookahead bayesian optimization. *Advances in neural information processing systems*, 32, 2019.
- [46] Donald R Jones, Cary D Perttunen, and Bruce E Stuckman. Lipschitzian optimization without the lipschitz constant. *Journal of optimization Theory and Applications*, 79(1):157–181, 1993.
- [47] Dong C Liu and Jorge Nocedal. On the limited memory bfgs method for large scale optimization. *Mathematical programming*, 45(1):503–528, 1989.
- [48] Alexander IJ Forrester, Andrés Sóbester, and Andy J Keane. Multi-fidelity optimization via surrogate modelling. *Proceedings of the royal society a: mathematical, physical and engineering sciences*, 463(2088):3251–3269, 2007.
- [49] Benjamin Peherstorfer, Karen Willcox, and Max Gunzburger. Survey of multifidelity methods in uncertainty propagation, inference, and optimization. *Siam Review*, 60(3):550–591, 2018.
- [50] Philip S Beran, Dean Bryson, Andrew S Thelen, Matteo Diez, and Andrea Serani. Comparison of multi-fidelity approaches for military vehicle design. In *AIAA AVIATION 2020 FORUM*, page 3158, 2020.
- [51] Alexander IJ Forrester, Andrés Sóbester, and Andy J Keane. Multi-fidelity optimization via surrogate modelling. *Proceedings of the royal society a: mathematical, physical and engineering sciences*, 463(2088):3251–3269, 2007.
- [52] Josyula Umakant, Krishnarao Sudhakar, PM Mujumdar, and C Raghavendra Rao. Ranking based uncertainty quantification for a multifidelity design approach. *Journal of aircraft*, 44(2):410–419, 2007.
- [53] Dev Rajnarayan, Alex Haas, and Ilan Kroo. A multifidelity gradient-free optimization method and application to aerodynamic design. In *12th AIAA/ISSMO multidisciplinary analysis and optimization conference*, page 6020, 2008.

- [54] Douglas Allaire, Karen Willcox, and Olivier Toupet. A bayesian-based approach to multifidelity multidisciplinary design optimization. In *13th AIAA/ISSMO multidisciplinary analysis optimization conference*, page 9183, 2010.
- [55] L Bonfiglio, P Perdikaris, S Brizzolara, and GE Karniadakis. Multi-fidelity optimization of super-cavitating hydrofoils. *Computer Methods in Applied Mechanics and Engineering*, 332:63–85, 2018.
- [56] Jialin Song, Yuxin Chen, and Yisong Yue. A general framework for multi-fidelity bayesian optimization with gaussian processes. In *The 22nd International Conference on Artificial Intelligence and Statistics*, pages 3158–3167. PMLR, 2019.
- [57] Mahdi Imani and Seyede Fatemeh Ghoreishi. Scalable inverse reinforcement learning through multifidelity bayesian optimization. *IEEE transactions on neural networks and learning systems*, 2021.
- [58] Jian Wu, Saul Toscano-Palmerin, Peter I Frazier, and Andrew Gordon Wilson. Practical multi-fidelity bayesian optimization for hyperparameter tuning. In *Uncertainty in Artificial Intelligence*, pages 788–798. PMLR, 2020.
- [59] Soumya Vasisht, Aowabin Rahman, Thiagarajan Ramachandran, Arnab Bhattacharya, and Veronica Adetola. Multi-fidelity bayesian optimization for co-design of resilient cyber-physical systems. In *2022 ACM/IEEE 13th International Conference on Cyber-Physical Systems (ICCPs)*, pages 298–299. IEEE, 2022.
- [60] Simone Pezzuto, Paris Perdikaris, and Francisco Sahli Costabal. Learning cardiac activation maps from 12-lead ecg with multi-fidelity bayesian optimization on manifolds. *arXiv preprint arXiv:2203.06222*, 2022.
- [61] Marc C Kennedy and Anthony O’Hagan. Predicting the output from a complex computer code when fast approximations are available. *Biometrika*, 87(1):1–13, 2000.
- [62] Xiongfeng Ruan, Ping Jiang, Qi Zhou, Jiexiang Hu, and Leshi Shu. Variable-fidelity probability of improvement method for efficient global optimization of expensive black-box problems. *Structural and Multidisciplinary Optimization*, 62(6):3021–3052, 2020.
- [63] Deng Huang, Theodore T Allen, William I Notz, and R Allen Miller. Sequential kriging optimization using multiple-fidelity evaluations. *Structural and Multidisciplinary Optimization*, 32(5):369–382, 2006.
- [64] Yehong Zhang, Trong Nghia Hoang, Bryan Kian Hsiang Low, and Mohan Kankanhalli. Information-based multi-fidelity bayesian optimization. In *NIPS Workshop on Bayesian Optimization*, 2017.
- [65] Shion Takeno, Hitoshi Fukuoka, Yuhki Tsukada, Toshiyuki Koyama, Motoki Shiga, Ichiro Takeuchi, and Masayuki Karasuyama. Multi-fidelity bayesian optimization with max-value entropy search and its parallelization. In *International Conference on Machine Learning*, pages 9334–9345. PMLR, 2020.
- [66] Francesco Di Fiore and Laura Mainini. Non-myopic multifidelity bayesian optimization. *arXiv preprint arXiv:2207.06325*, 2022.
- [67] Naoki Abe. Query learning strategies using boosting and bagging. *Proc. of 15<sup>th</sup> Int. Conf. on Machine Learning (ICML98)*, pages 1–9, 1998.
- [68] Robert Burbidge, Jem J Rowland, and Ross D King. Active learning for regression based on query by committee. In *International conference on intelligent data engineering and automated learning*, pages 209–218. Springer, 2007.
- [69] Wenbin Cai, Muhan Zhang, and Ya Zhang. Batch mode active learning for regression with expected model change. *IEEE transactions on neural networks and learning systems*, 28(7):1668–1681, 2016.
- [70] Beguem Demir and Lorenzo Bruzzone. A multiple criteria active learning method for support vector regression. *Pattern recognition*, 47(7):2558–2567, 2014.
- [71] Tirthankar RayChaudhuri and Leonard GC Hamey. Minimisation of data collection by active learning. In *Proceedings of ICNN’95-International Conference on Neural Networks*, volume 3, pages 1338–1341. IEEE, 1995.
- [72] Burr Settles and Mark Craven. An analysis of active learning strategies for sequence labeling tasks. In *proceedings of the 2008 conference on empirical methods in natural language processing*, pages 1070–1079, 2008.
- [73] H Sebastian Seung, Manfred Opper, and Haim Sompolinsky. Query by committee. In *Proceedings of the fifth annual workshop on Computational learning theory*, pages 287–294, 1992.
- [74] Dongrui Wu. Pool-based sequential active learning for regression. *IEEE transactions on neural networks and learning systems*, 30(5):1348–1359, 2018.
- [75] Masashi Sugiyama and Shinichi Nakajima. Pool-based active learning in approximate linear regression. *Machine Learning*, 75(3):249–274, 2009.

- [76] Tianxu He, Shukui Zhang, Jie Xin, Pengpeng Zhao, Jian Wu, Xuefeng Xian, Chunhua Li, and Zhiming Cui. An active learning approach with uncertainty, representativeness, and diversity. *The Scientific World Journal*, 2014, 2014.
- [77] Dan Shen, Jie Zhang, Jian Su, Guodong Zhou, and Chew Lim Tan. Multi-criteria-based active learning for named entity recognition. In *Proceedings of the 42nd annual meeting of the Association for Computational Linguistics (ACL-04)*, pages 589–596, 2004.
- [78] Dongrui Wu, Vernon J Lawhern, Stephen Gordon, Brent J Lance, and Chin-Teng Lin. Offline eeg-based driver drowsiness estimation using enhanced batch-mode active learning (ebmal) for regression. In *2016 IEEE International Conference on Systems, Man, and Cybernetics (SMC)*, pages 000730–000736. IEEE, 2016.
- [79] Robert Munro Monarch. *Human-in-the-Loop Machine Learning: Active learning and annotation for human-centered AI*. Simon and Schuster, 2021.
- [80] Xueying Zhan, Huan Liu, Qing Li, and Antoni B Chan. A comparative survey: Benchmarking for pool-based active learning. In *IJCAI*, pages 4679–4686, 2021.
- [81] David D Lewis and Jason Catlett. Heterogeneous uncertainty sampling for supervised learning. In *Machine learning proceedings 1994*, pages 148–156. Elsevier, 1994.
- [82] Maria-Florina Balcan, Andrei Broder, and Tong Zhang. Margin based active learning. In *International Conference on Computational Learning Theory*, pages 35–50. Springer, 2007.
- [83] Mingkun Li and Ishwar K Sethi. Confidence-based active learning. *IEEE transactions on pattern analysis and machine intelligence*, 28(8):1251–1261, 2006.
- [84] Alex Holub, Pietro Perona, and Michael C Burl. Entropy-based active learning for object recognition. In *2008 IEEE Computer Society Conference on Computer Vision and Pattern Recognition Workshops*, pages 1–8. IEEE, 2008.
- [85] David Cohn. Neural network exploration using optimal experiment design. *Advances in neural information processing systems*, 6, 1993.
- [86] Wenbin Cai, Ya Zhang, and Jun Zhou. Maximizing expected model change for active learning in regression. In *2013 IEEE 13th international conference on data mining*, pages 51–60. IEEE, 2013.
- [87] Yue Zhao, Ciwen Xu, and Yongcun Cao. Research on query-by-committee method of active learning and application. In *International Conference on Advanced Data Mining and Applications*, pages 985–991. Springer, 2006.
- [88] Sanjoy Dasgupta and Daniel Hsu. Hierarchical sampling for active learning. In *Proceedings of the 25th international conference on Machine learning*, pages 208–215, 2008.
- [89] Ozan Sener and Silvio Savarese. A geometric approach to active learning for convolutional neural networks. *arXiv preprint arXiv:1708.00489*, 7, 2017.
- [90] Rita Chattopadhyay, Zheng Wang, Wei Fan, Ian Davidson, Sethuraman Panchanathan, and Jieping Ye. Batch mode active sampling based on marginal probability distribution matching. *ACM Transactions on Knowledge Discovery from Data (TKDD)*, 7(3):1–25, 2013.
- [91] Yifan Fu, Bin Li, Xingquan Zhu, and Chengqi Zhang. Active learning without knowing individual instance labels: a pairwise label homogeneity query approach. *IEEE Transactions on Knowledge and Data Engineering*, 26(4):808–822, 2013.
- [92] Tobias Reitmaier, Adrian Calma, and Bernhard Sick. Transductive active learning—a new semi-supervised learning approach based on iteratively refined generative models to capture structure in data. *Information Sciences*, 293:275–298, 2015.
- [93] Yu Zhao, Zhenhui Shi, Jingyang Zhang, Dong Chen, and Lixu Gu. A novel active learning framework for classification: Using weighted rank aggregation to achieve multiple query criteria. *Pattern Recognition*, 93:581–602, 2019.
- [94] Wei-Ning Hsu and Hsuan-Tien Lin. Active learning by learning. In *Twenty-Ninth AAAI conference on artificial intelligence*, 2015.
- [95] Xin Li and Yuhong Guo. Adaptive active learning for image classification. In *Proceedings of the IEEE conference on computer vision and pattern recognition*, pages 859–866, 2013.
- [96] Zheng Wang and Jieping Ye. Querying discriminative and representative samples for batch mode active learning. *ACM Transactions on Knowledge Discovery from Data (TKDD)*, 9(3):1–23, 2015.

- [97] Ying-Peng Tang and Sheng-Jun Huang. Self-paced active learning: Query the right thing at the right time. In *Proceedings of the AAAI conference on artificial intelligence*, volume 33, pages 5117–5124, 2019.
- [98] J Mockus. On the bayes methods for seeking the extremal point. *IFAC Proceedings Volumes*, 8(1):428–431, 1975.
- [99] Donald R Jones. A taxonomy of global optimization methods based on response surfaces. *Journal of global optimization*, 21(4):345–383, 2001.
- [100] Quoc Phong Nguyen, Bryan Kian Hsiang Low, and Patrick Jaillet. Rectified max-value entropy search for bayesian optimization. *arXiv preprint arXiv:2202.13597*, 2022.
- [101] Pinar Donmez and Jaime G Carbonell. Proactive learning: cost-sensitive active learning with multiple imperfect oracles. In *Proceedings of the 17th ACM conference on Information and knowledge management*, pages 619–628, 2008.
- [102] Chicheng Zhang and Kamalika Chaudhuri. Active learning from weak and strong labelers. *Advances in Neural Information Processing Systems*, 28, 2015.
- [103] Songbai Yan, Kamalika Chaudhuri, and Tara Javidi. Active learning from imperfect labelers. *Advances in Neural Information Processing Systems*, 29, 2016.
- [104] Liyue Zhao, Gita Sukthankar, and Rahul Sukthankar. Incremental relabeling for active learning with noisy crowdsourced annotations. In *2011 IEEE third international conference on privacy, security, risk and trust and 2011 IEEE third international conference on social computing*, pages 728–733. IEEE, 2011.
- [105] Pinar Donmez, Jaime G Carbonell, and Jeff Schneider. Efficiently learning the accuracy of labeling sources for selective sampling. In *Proceedings of the 15th ACM SIGKDD international conference on Knowledge discovery and data mining*, pages 259–268, 2009.
- [106] Panagiotis G Ipeirotis, Foster Provost, Victor S Sheng, and Jing Wang. Repeated labeling using multiple noisy labelers. *Data Mining and Knowledge Discovery*, 28(2):402–441, 2014.
- [107] Yan Yan, Romer Rosales, Glenn Fung, and Jennifer G Dy. Active learning from crowds. In *ICML*, 2011.
- [108] Yan Yan, Rómer Rosales, Glenn Fung, Faisal Farooq, Bharat Rao, and Jennifer Dy. Active learning from multiple knowledge sources. In *Artificial Intelligence and Statistics*, pages 1350–1357. PMLR, 2012.
- [109] Meng Fang, Jie Yin, and Dacheng Tao. Active learning for crowdsourcing using knowledge transfer. In *Proceedings of the AAAI Conference on Artificial Intelligence*, volume 28, 2014.
- [110] Sheng-Jun Huang, Jia-Lve Chen, Xin Mu, and Zhi-Hua Zhou. Cost-effective active learning from diverse labelers. In *IJCAI*, pages 1879–1885, 2017.
- [111] Guoxian Yu, Xia Chen, Carlotta Domeniconi, Jun Wang, Zhao Li, Zili Zhang, and Xiangliang Zhang. Cmal: Cost-effective multi-label active learning by querying subexamples. *IEEE Transactions on Knowledge and Data Engineering*, 2020.
- [112] Ruijiang Gao and Maytal Saar-Tsechansky. Cost-accuracy aware adaptive labeling for active learning. In *Proceedings of the AAAI Conference on Artificial Intelligence*, volume 34, pages 2569–2576, 2020.
- [113] Yixin Liu, Shishi Chen, Fenggang Wang, and Fenfen Xiong. Sequential optimization using multi-level cokriging and extended expected improvement criterion. *Structural and Multidisciplinary Optimization*, 58(3):1155–1173, 2018.
- [114] Michael D McKay. Latin hypercube sampling as a tool in uncertainty analysis of computer models. In *Proceedings of the 24th conference on Winter simulation*, pages 557–564, 1992.
- [115] András Sobester, Alexander Forrester, and Andy Keane. *Engineering design via surrogate modelling: a practical guide*. John Wiley & Sons, 2008.
- [116] Markus P Rumpfkeil and Philip S Beran. Multi-fidelity, gradient-enhanced, and locally optimized sparse polynomial chaos and kriging surrogate models applied to benchmark problems. In *AIAA Scitech 2020 Forum*, page 0677, 2020.
- [117] Handing Wang, Yaochu Jin, and John Doherty. A generic test suite for evolutionary multifidelity optimization. *IEEE Transactions on Evolutionary Computation*, 22(6):836–850, 2017.
- [118] Daniel L Clark Jr, Ha-Rok Bae, Koorosh Gobal, and Ravi Penmetsa. Engineering design exploration using locally optimized covariance kriging. *AIAA Journal*, 54(10):3160–3175, 2016.
- [119] David JJ Toal. Some considerations regarding the use of multi-fidelity kriging in the construction of surrogate models. *Structural and Multidisciplinary Optimization*, 51(6):1223–1245, 2015.

- [120] Andrea Serani, Cecilia Leotardi, Umberto Iemma, Emilio F Campana, Giovanni Fasano, and Matteo Diez. Parameter selection in synchronous and asynchronous deterministic particle swarm optimization for ship hydrodynamics problems. *Applied Soft Computing*, 49:313–334, 2016.